# Energy-efficient train control using nonlinear bounded regenerative braking

Scheepmaker, Gerben M.; Goverde, Rob M.P.

**Important note**
To cite this publication, please use the final published version (if applicable).
Please check the document version above.
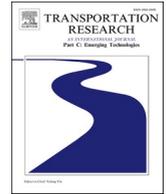
# Energy-efficient train control using nonlinear bounded regenerative braking

Gerben M. Scheepmaker [a,b,*], Rob M.P. Goverde [a]

[a] *Department of Transport and Planning, Delft University of Technology, P.O. Box 5048, 2600 GA Delft, The Netherlands*
[b] *Netherlands Railways, Department of Performance Management and Innovation, P.O. Box 2025, 3500 HA Utrecht, The Netherlands*

A B S T R A C T

*Energy-efficient train control* (*EETC*) has been studied a lot over the last decades, because it contributes to cost savings and reduction of $CO_2$ emissions. The aim of EETC is to minimize total traction energy consumption of a train run given the running time in the timetable. Most research is focused to apply *mechanical braking* on this problem. However, current trains are able to use *regenerative braking*, which leads to another optimal driving strategy compared to mechanical braking. Research on EETC with a realistic nonlinear bounded model for regenerative braking or a combination between regenerative and mechanical braking is limited. The aim of this paper is to compare the difference between the EETC with regenerative and/or mechanical braking. First, we derive the optimal control structure for the problems with different braking combinations. Second, we apply the pseudospectral method on different scenarios where we investigate the effect of varying speed limits and gradients on the different driving strategies. Results indicate that compared to pure mechanical braking, combined regenerative and mechanical braking leads to a driving strategy with higher energy savings, a lower optimal cruising speed, a shorter coasting phase and a higher speed at the beginning of the braking phase. In addition, a nonlinear bounded regenerative braking curve leads to a different driving strategy compared to a constant braking rate that is commonly used in literature. We show that regenerative braking at a constant braking rate overestimates the total energy savings.

## 1. Introduction

The topic of *energy-efficient train control* (*EETC*) or *energy-efficient train trajectory optimization* has been studied a lot in the literature during the last decades. The aim of EETC is to run a train with the least traction energy consumption. Therefore, the train uses the available *running time supplements* in order to arrive exactly on-time (i.e. not too early and not too late) at the next station. The running time supplements are the extra running times above the minimum-time running in order to cope with small delays or to deal with disturbances during operations. The minimum-time running can be computed by solving the *minimum-time train control* (*MTTC*) problem. Energy-efficient train driving is applied if the train is running punctual (Scheepmaker and Goverde, 2015). A comprehensive overview on the topic of energy-efficient train control can be found in Scheepmaker et al. (2017) and Yang et al. (2016).

The EETC problem can be formulated as an optimal control problem. By using *Pontryagin's Maximum Principle* (*PMP*) the optimal

control can be shown to consist of the optimal driving regimes maximum acceleration (MA), cruising (CR), coasting (CO) and maximum braking (MB) (Howlett and Pudney, 1995; Khmelnitsky, 2000; Liu and Golovitcher, 2003; Albrecht et al., 2016a; Albrecht et al., 2016b). The challenge is to derive the optimal order of the driving regimes and the switching points between them. For more details on this topic we refer to Scheepmaker et al. (2017).

Modern trains have the possibility to apply both *mechanical braking* and *regenerative braking*. Braking disks or pads are used in order to convert kinetic energy into heat, while applying mechanical braking. During regenerative braking electricity is generated while using the engine of the train as a generator in order to convert the kinetic energy into electricity. This electricity can be used for the train itself such as heating or lighting, stored within batteries or it can be fed back to the catenary system for other surrounding trains. For urban rail relatively more energy savings can be achieved by energy storage compared to utilizing the regenerated energy by surrounding trains (González-Gil et al., 2014). In this paper we focus on the utilization of regenerated braking energy by surrounding trains for heavy rail, because a lot of research on regenerative braking is considering the topic of synchronizing accelerating and regenerative braking trains including energy-efficient train control (Scheepmaker et al., 2017). For more details about regenerative braking and different regenerative braking storage techniques for urban rail systems, we refer to the review paper of González-Gil et al. (2013).

The topic of regenerative braking has been studied both for multiple-trains as well as single trains (Scheepmaker et al., 2017). In the multiple train problem, the aim is to synchronize accelerating and regenerative braking trains, in order to maximize the usage of regenerative braking. This leads to the energy-efficient train timetable (EETT) problem that determines the optimal departure and arrival times within stations, which is mainly focused on urban railway networks. Examples of the EETT problem with regenerative braking can be found in Albrecht et al. (2004), Peña-Alcaraz et al. (2012), Yang et al. (2013), Yang et al. (2014), Li and Lo (2014a), Li and Lo (2014b), Zhou et al. (2018), Luan et al. (2018a,b). In the single-train problem, the aim is to find the energy-efficient train control with regenerative braking, so the objective function includes regenerated energy during braking, which depends on the efficiency of the regenerative braking system. Asnis et al. (1985) started this research by considering flat tracks. The main difference between the EETC models with mechanical braking is that the driving regimes with mechanical braking are replaced by regenerative braking, such as cruising by partial braking and maximum braking. Later studies include varying gradients and speed limits. Khmelnitsky (2000) and Franke et al. (2000) both used time and energy as state variables to derive analytical expressions for the different driving regimes for the EETC problem including regenerative braking. Moreover, Albrecht et al. (2016a,b) discussed the key principles of optimal train control with regenerative braking using continuous control settings and included speed limits and steep gradients. They generalized the formulations of traction and regenerative braking control by using monotone functions and a generic function for the train resistance. Qu et al. (2014) focused on the optimal cruising speed and regenerative braking for metro trains, where they excluded coasting. In the European project ON-TIME (Optimal Networks for Train Integration Management across Europe) an iterative gradient-based algorithm was developed to determine the energy-efficient driving strategy including regenerative braking that can be used for a Driver Advisory System (DAS) (ON-TIME, 2014). Yang et al. (2018) developed an analytical method to determine the optimal train control for a complete metro line, by subdividing the trajectory in phases with constant speed limits. They included the effect of regenerative braking in order to minimize the total energy consumption, but varying gradients were not considered in their model. Their train control method was part of an optimization method that determined the energy-optimal timetable for a single train for a complete metro line.

The main assumption behind the discussed papers is that they consider regenerative braking only, and assumed it as constant. In practice trains need mechanical braking as well, since the regenerative braking force is limited by the maximum regenerative braking force and the power of the engine (given by the traction/regenerative braking force diagram) (Frilli et al., 2016; Zhou et al., 2018). This is especially the case for high speeds where the power of the traction engine is limited as well as speeds close to zero, where mechanical braking is applied to compensate the total braking force. Up to our knowledge, only Baranov et al. (2011), Lu et al. (2014), Fernández-Rodríguez et al. (2018), Zhou et al. (2018) investigated the combination of mechanical and regenerative braking. Baranov et al. (2011) considered traction, regenerative braking and mechanical braking. They considered the seven optimal driving regimes including two driving regimes for the combination of regenerative and mechanical braking (i.e., cruising by partial regenerative braking (CR2), maximum regenerative braking (MRB), cruising by maximum regenerative and partial mechanical braking (CR3), and maximum total braking (MB)). However, the derivation of these regimes as well as an algorithm to solve the optimal sequence of the driving regimes was not provided. Lu et al. (2014) only considered the braking part of the trajectory optimization in order to maximize the regenerative braking energy. They made a distinction between mechanical and regenerative braking and they compared the difference between a constant braking rate (or mass-specific train braking force) and the regenerative braking rate depending on the maximum regenerative braking force and the regenerative braking power. Using PMP they derived four regimes consisting of coasting, cruising by braking, maximum regenerative braking, and maximum total braking, but without considering varying speed limits and varying gradients. Fernández-Rodríguez et al. (2018) considered a dynamic multi-objective optimization model to compute the optimal speed profiles during train driving for high speed trains that minimize total delay and energy consumption. The energy-efficient speed profiles are determined by using a simulation model for the train motion and includes both mechanical and regenerative braking. However, the optimal structure of the speed profiles with the different driving regimes and switching points as well as the comparison between the simulation results and optimal control theory were not discussed in this paper. Moreover, the model results only show where the train is braking, but not if the train applies regenerative and/or mechanical braking. Zhou et al. (2018) developed an integrating model for the train control and timetable optimization in order to minimize the total net energy consumption by synchronizing accelerating and regenerative braking trains. They included the combination of regenerative and mechanical braking and solved train control and the timetabling problem using heuristics. However, they considered the four driving regimes (MA, CR, CO and MB) without the derivation of these regimes, and they did not include varying speed limits. Scheepmaker and Goverde (2016) and Scheepmaker et al. (2020)

compared the difference of EETC between regenerative braking only and mechanical braking only, but they did not consider the combination of regenerative and mechanical braking and they applied the comparison of the different EETC braking strategies only on flat track. Scheepmaker et al. (2020) included varying speed limits. Most research assumes a constant value for the efficiency of the train due to power losses (i.e. efficiency of the engine). However, Ghaviha et al. (2017) investigated the effect of a dynamic efficiency on the energy-efficient train control problem with regenerative braking that considers the losses due to the inverter, motor and gearbox that sum up to the dynamic total power loss. This leads to a more realistic calculations of the energy consumption of the train and the computed speed profile is more energy-efficient compared to models using a constant efficiency factor. For battery catenary-free electric trains Ghaviha et al. (2019) combine the single mass point mechanical train control model with the electrical train battery model, and indicate that these trains should focus on minimizing the total charge of the battery during catenary-free operation.

The aim of this paper is to derive the energy-efficient train control with both mechanical and regenerative braking and to apply them within a model on numerical examples including varying speed limits and varying gradients. Therefore, the paper gives the following contributions to the literature:

1. We consider an optimal train control problem with three control variables (traction, regenerative braking and mechanical braking).
2. We consider the effect of the actual nonlinear bounded regenerative braking constraints and compare this to the commonly used constant regenerative braking on the energy-efficient train control.
3. We derive the optimal energy-efficient train control with nonlinear bounded regenerative braking and/or mechanical braking.
4. We apply a pseudospectral method considering the EETC problem with a variation of regenerative and/or mechanical braking on different numerical realistic experiments with various scenarios to show their difference.

The paper outline is as follows. Section 2 provides the optimal train control problem for both EETC and MTTC including the necessary optimality conditions. Section 3 explains briefly the pseudospectral method applied in this paper. In order to show the working of the multiple-phase pseudospectral method, a case study is presented in Section 4 based on Dutch infrastructure and rolling stock data. Finally, the conclusions are provided in Section 5.

## 2. Optimal train control problem

This section gives the optimal train control problem formulation and a derivation of the necessary optimality conditions by applying Pontryagin's Maximum Principle (Lewis et al., 2012; Ross, 2015). These conditions provide a formal derivation of the optimal driving regimes when considering a mixture of mechanical and regenerative braking. We consider both mechanical and regenerative braking like Baranov et al. (2011) and model the train as a point mass (Brünger et al., 2014; Howlett and Pudney, 1995). Moreover, we use time as independent variable. We follow a similar derivation of the necessary optimality conditions for the optimal train control problem as Howlett (2000), Khmelnitsky (2000), Liu and Golovitcher (2003), Albrecht et al. (2016a, 2016b), Goverde et al. (2020). However, since we include both regenerative and mechanical braking our problem formulation is different. We use the step-wise optimal control analysis and separate the specific control $u$ into specific traction $f$, specific regenerative braking $b_r$ and specific mechanical braking $b_m$ (i.e. $u = f + b_r + b_m$). Therefore, for the case of both regenerative and mechanical braking, the problem
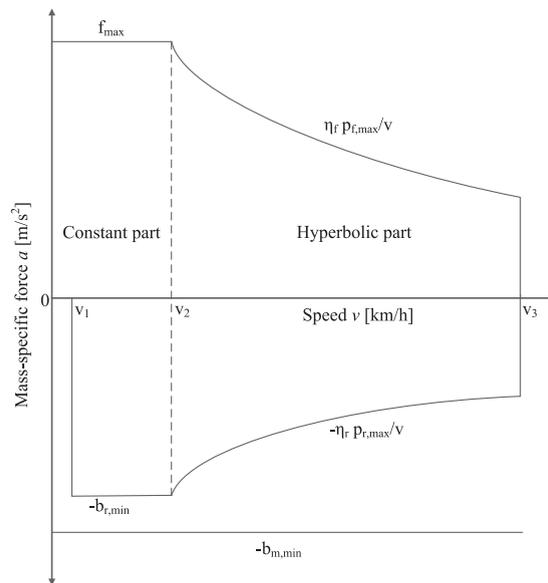


**Fig. 1.** Typical mass-specific traction-speed ($f$) and mass-specific regenerative braking-speed ($b_r$) diagram with a constant and hyperbolic part, and a constant mass-specific mechanical braking force $b_m$. The mass-specific regenerative braking force is zero below speed $v_1$.

formulation is comparable to Baranov et al. (2011).

First, Section 2.1 explains the concept of regenerative braking more in depth. Afterwards, Section 2.2 gives the energy-efficient train control problem including both regenerative and mechanical braking. Third, regenerative braking only for EETC is considered in Section 2.3. Fourth, mechanical braking only for the EETC problem is discussed in Section 2.4. Finally, the minimum-time train control (MTTC) problem is considered in Section 2.5 where both mechanical and regenerative braking can be applied.

### 2.1. Regenerative braking

The electric engine of a train can be used both for traction and dynamic braking (González-Gil et al., 2013; Lu et al., 2014). During dynamic braking the electric engine of the train is used to convert dynamic energy into electric energy by using the opposite direction of the torque of the motor compared to the rotating speed. This electric energy can be converted into heat using various resistors, which is called rheostatic braking, or it can be used for the train itself (such as heating or air conditioning), stored in energy storage systems or send to other trains by transmitting the electricity over the catenary system, which is called regenerative braking. In this paper we focus on regenerative braking where the regenerated energy is transformed into electricity that can be used for other surrounding trains. Since the train uses the electric motor (engine) as a generator during regenerative braking, the regenerative force is bounded by the performance of the engine like the traction force, which can be visualized in the traction/braking force diagram, see Fig. 1. The traction force has a constant part in which the maximum traction force is limiting the maximum traction force (overheat and adhesion limit) and a hyperbolic part, where the power is limiting the maximum traction force (Steimel, 2008; Brünger et al., 2014). During regenerative braking the same engine is used, therefore, the maximum regenerative force is limited by a constant part (maximum regenerative braking force) and a hyperbolic part (maximum regenerative braking power). In addition, during low speeds regenerative braking cannot be applied, because of the limited kinetic energy that can be converted into energy (low current produced) and it should overcome the power losses in the engine and over the catenary (Pengyu et al., 2009; Yi, 2018). Therefore, trains in practice apply just mechanical braking at speeds below some speed $v_1$ (close to zero). In this paper we use the rolling stock data of VIRM-6 of the Netherlands Railways (NS) in the case study which applies zero regenerative braking force below speed $v_1 = 8$ km/h (NS, 2020), see Table 1. Finally, we assume that the regenerated energy can be used by another accelerating train and that it is not used by or stored in the train itself, so we consider the regenerative braking energy flow to the engine of the other accelerating train. In addition, we focus on the trajectory optimization of a single train. In practice the utilization of regenerative braking energy by surrounding trains depends on a series of factors such as the operation mode of surrounding trains, the distance between the synchronized accelerating and regenerative braking trains, and the maximum allowable voltage of the power supply system. Including these different aspects requires detailed modelling of the power supply system over the catenary, which requires simulation models such as OpenPowerNet (Stephan, 2008). Our paper focuses on the effect of the actual nonlinear bounded regenerative braking instead of the commonly used constant regenerative braking on the energy-efficient train control. In future work, our train control model can be embedded within a complex electricity simulation model to obtain dynamic condition-dependent estimated parameters of the catenary and the receiving train.

### 2.2. Energy-efficient train control with nonlinear bounded regenerative and mechanical braking (RMeB)

In this section we consider the energy-efficient train control problem including regenerative and mechanical braking. The aim for energy-efficient train control is to minimize total mass-specific traction energy $E$ [m$^2$/s$^2$] between two consecutive stops over the total distance $S$ [m] given the scheduled running time $T$ [s] (with sufficient running time supplement) according to the timetable:

$$E = \min \int_0^T \left( f\left(t\right) + \eta b_r\left(t\right) \right) v\left(t\right) dt, \tag{1}$$

**Table 1**
Basic parameters of a NS Intercity train rolling stock type VIRM-6 (NS, 2020).

| Property | Notation | Value |
|---|---|---|
| Train mass [t] | $m$ | 391 |
| Rotating mass supplement [%] | $\rho$ | 6 |
| Maximum traction power [kW] | $P_e$ | 2157 |
| Maximum regenerative power [kW] | $P_r$ | 3616 |
| Maximum traction force [kN] | $F$ | 213.9 |
| Maximum regenerative braking force [kN] | $-B_{r,\min}$ | −142.5 |
| Maximum mechanical braking force [kN] | $-B_{m,\min}$ | −273.5 |
| Maximum braking deceleration [m/s$^2$] | $-b_{\min}$ | −0.66 |
| Minimum speed limit for regenerative braking [km/h] | $v_1$ | 8 |
| Maximum speed limit [km/h] | $v_{\max}$ | 140 |
| Train resistance [kN] (v: [km/h]) | $R$ | $5.8584 + 0.0206v + 0.001v^2$ |
| Efficiency of the engine [%] | $\eta_f, \eta_r, \eta_s$ | 87.5 |
| Catenary efficiency 1.5 kV DC [%] | $\eta_c$ | 80.0 |

subject to the constraints

$$\dot{s}(t) = v(t) \tag{2}$$

$$\dot{v}(t) = f(t) + b_r(t) + b_m(t) - r(v) - g(s) \tag{3}$$

$$f(t)v(t) \leqslant \eta_f p_{f,\max} \tag{4}$$

$$-b_r(t)v(t) \leqslant \eta_r p_{r,\max} \tag{5}$$

$$0 \leqslant v(t) \leqslant v_{\max}(s) \tag{6}$$

$$0 \leqslant f(t) \leqslant f_{\max} \tag{7}$$

$$-b_{r,\min} \leqslant b_r(t) \leqslant 0 \tag{8}$$

$$b_r(t) = 0 \text{ if } v(t) < v_1 \tag{9}$$

$$-b_{m,\min} \leqslant b_m(t) \leqslant 0 \tag{10}$$

$$b_r + b_m \leqslant b_{\min} \tag{11}$$

$$s(t_0) = 0, s(t_f) = S, v(t_0) = 0, v(t_f) = 0, \tag{12}$$

where time $t$ [s] is defined as the independent variable, distance $s$ [m] and speed $v$ [m/s] are the state variables, the derivatives of the state variables to the independent variable are $\dot{x} = dx/dt$ and $\dot{v} = dv/dt$, and the control variables are mass-specific traction force $f$ [m/s$^2$], mass-specific (positive) regenerative braking force $b_r$ [m/s$^2$], and mass-specific (positive) mechanical braking force $b_m$ [m/s$^2$]. Moreover, the total mass-specific braking force is defined by the combination of regenerative and mechanical braking, i.e. $b(t) = b_r(t) + b_m(t)$, which is bounded by the maximum mass-specific braking force $b_{\min}$. The mass-specific traction, regenerative braking and mechanical braking force are defined by the total force (traction force $F$ [N], regenerative braking force $B_r$ [N] and mechanical braking force $B_m$ [N]) divided by the total rotating mass (i.e. train mass $m$ [kg] multiplied by rotating mass factor $\rho$ [–]), thus $f = F(t)/(\rho m)$, $b_r = B_r(t)/(\rho m)$ and $b_m = B_m(t)/(\rho m)$. The mass-specific traction force is bounded by $f_{\max}$, the mass-specific regenerative braking force is bounded by $-b_{r,\min}$, and the mass-specific mechanical braking force is bounded by $-b_{m,\min}$. The regenerative braking and mechanical braking are independent of each other and add up to the total braking. The maximum total mass-specific braking force is limited for passenger comfort to $b_{\min}$ as stated in (11). The traction and regenerative braking forces are functions of speed and consist of a constant part (depending on the maximum traction or regenerative braking force) and a hyperbolic part that depends on traction efficiency $\eta_f$ [-] or regenerative braking efficiency $\eta_r$ [-] and the specific power $p$ [m$^2$/s$^3$] of the train, see Fig. 1. Furthermore, regenerative braking cannot be applied below the speed $v_1$ as explained in Section 2.1. The total efficiency for regenerative braking energy $\eta$ [-] depends on the efficiency of the engine of the train during regenerative braking $\eta_r$ [-], the efficiency of the catenary $\eta_c$ [-], and the efficiency of the engine of the second train during acceleration $\eta_s$ [-], i.e. $\eta = \eta_r \eta_c \eta_s$. The specific power is limited by the maximum specific power $p_{\max}$. Therefore, the traction control is bounded by $f \leqslant f_{\max}(v) = \min(f_{\max}, \eta_f p_{f,\max}/v)$ and the regenerative braking control is bounded by $b_r \geqslant b_{r,\min}(v) = -\min(b_{r,\min}, \eta_r p_{r,\max}/v)$. Note that we explicitly consider both the efficiency of the traction control $\eta_f$ and regenerative braking control $\eta_r$ while in literature this is mostly modelled implicitly in the maximum power (e.g. Scheepmaker et al. (2020)). Moreover, traction and braking control (both regenerative and mechanical) cannot be applied at the same time, i.e. $f \cdot (b_r + b_m) = 0$. The total mass-specific train resistance consists of the mass-specific train resistance $r(v)$ [m/s$^2$] and the mass-specific line resistance $g(s)$ [m/s$^2$]. The mass-specific train resistance is defined by Davis equation $r(v) = r_0 + r_1 v + r_2 v^2$, where $r_0, r_1 \geqslant 0$ and $r_2 > 0$ are non-negative coefficients (Davis, 1926). The mass-specific line resistance is caused by varying gradients, where $g(s) > 0$ denotes uphill slopes and $g(s) < 0$ downhill slopes. We assume a piecewise constant speed limit $v_{\max}(s)$ and gradient $g(s)$ over distance. Finally, the difference in the optimal control problem formulation given in (1)–(12) with current literature is that we include the combination of mechanical and regenerative braking in (3) and (11) and we consider the nonlinear bounded maximum regenerative braking behavior in (5) (i.e. regenerative braking-speed diagram given in Fig. 1).

With the problem formulation it is now possible to derive the necessary optimality conditions. We start with defining the Hamiltonian $H$ [m$^2$/s$^3$] as

$$H(s, v, \lambda_1, \lambda_2, f, b_r, b_m) = (\lambda_2 - v)f + (\lambda_2 - \eta v)b_r + \lambda_2 b_m + \lambda_1 v - \lambda_2 r(v) - \lambda_2 g(s), \tag{13}$$

where the costate variables are defined by $\lambda_1(t)$ [m/s$^2$] and $\lambda_2(t)$ [m/s] as functions of the independent variable $t$. Moreover, the Hamiltonian is independent of time and so $\partial H/\partial t = 0$. Next, the augmented Hamiltonian $\overline{H}$ [m$^2$/s$^3$] also takes the additional (mixed) state and control path constraints (4)–(10) into account which leads to

$$\overline{H}\left(s, v, \lambda_1, \lambda_2, \mu, f, b_r, b_m\right) = H + \mu_1\left(f_{\max} - f\right) + \mu_2\left(b_r + b_{r,\min}\right) + \mu_3\left(b_m + b_{m,\min}\right) + \mu_4\left(b_{\min} - \left(b_r + b_m\right)\right)$$
$$+ \mu_5\left(\eta_f p_{f,\max} - fv\right) + \mu_6\left(\eta_r p_{r,\max} + b_r v\right) + \mu_7\left(v_{\max} - v\right), \tag{14}$$

with the nonnegative Lagrange multipliers $\mu_1$ [m/s], $\mu_2$ [m/s], $\mu_3$ [m/s], $\mu_4$ [m/s], $\mu_5$ [-], $\mu_6$ [-], $\mu_7$ [m/s$^2$]. The costates satisfy the differential equations $\dot{\lambda}_1(t) = -\partial \overline{H}/\partial s$ and $\dot{\lambda}_2(t) = -\partial \overline{H}/\partial v$ which gives

$$\dot{\lambda}_1(t) = \lambda_2 g'(s) \tag{15}$$

$$\dot{\lambda}_2(t) = f + \eta b_r - \lambda_1 + \lambda_2 r'(v) + \mu_5 f - \mu_6 b_r + \mu_7. \tag{16}$$

Note that the derivative of the gradients $g'(s)$ is almost everywhere zero, when the gradient is constant. Therefore, (15) indicates that $\lambda_1$ is constant when the gradients are constant. We can now apply Pontryagin's Maximum Principle on the optimal control, which states that the Hamiltonian should be maximized (Pontryagin et al., 1962). We define $U = [0, \min(f_{\max}, \eta_f p_f / v)] \times [-\min(b_{r,\min}, \eta_r p_r / v, 0), 0] \times [-b_{m,\min}, 0]$. The optimal controls $\widehat{f}(t)$, $\widehat{b}_r(t)$ and $\widehat{b}_m(t)$ are then defined by:

$$\left(\widehat{f}\left(t\right), \widehat{b}_r\left(t\right), \widehat{b}_m\left(t\right)\right) = \arg \max_{(f, b_r, b_m) \in U} H\left(\widehat{s}\left(t\right), \widehat{v}\left(t\right), \widehat{\lambda}_1\left(t\right), \widehat{\lambda}_2\left(t\right), f, b_r, b_m\right), \tag{17}$$

where $(\widehat{s}, \widehat{v})$ and $(\widehat{\lambda}_1, \widehat{\lambda}_2)$ are the state and costate trajectories associated to the optimal control trajectories $\widehat{f}$, $\widehat{b}_r$ and $\widehat{b}_m$. The Hamiltonian $H$ is linear in the controls $f$, $b_r$ and $b_m$ with coefficients $\lambda_2 - v$ for $f$, $\lambda_2 - \eta v$ for $b_r$, and $\lambda_2$ for $b_m$. Therefore, the value of the speed $v$ relative to the costate $\lambda_2$ determines the optimal controls $f$, $b_r$ and $b_m$ that maximize the Hamiltonian. This results in the following seven cases:

1. If $\lambda_2 > v$ then $f$ must be maximal (i.e., $f = \min(f_{\max}, \eta_f p_{f,\max}/v)$), and $b_r = b_m = 0$.
2. If $\lambda_2 = v$ then $f \in [0, \min(f_{\max}, \eta_f p_{f,\max}/v)]$ is undetermined (first singular solution), and $b_r = b_m = 0$.
3. If $\eta v < \lambda_2 < v$ then $f = b_r = b_m = 0$.
4. If $\lambda_2 = \eta v$ then $b_r \in [-\min(b_{r,\min}, \eta_r p_{r,\max}/v), 0]$ is undetermined (second singular solution), $f = 0$, and $b_m = 0$.
5. If $0 < \lambda_2 < \eta v$ then $b_r$ must be minimal (i.e., $b_{r,\min} = -\min(b_{r,\min}, \eta_r p_{r,\max}/v)$), $f = 0$, and $b_m = 0$.
6. If $\lambda_2 = 0$ then $b_m \in [-b_{m,\min}, 0]$ is undetermined (third singular solution) and $b_r$ must be minimal (i.e., $b_r = -\min(b_{r,\min}, \eta_r p_{r,\max}/v)$), and $f = 0$.
7. If $\lambda_2 < 0$ then $b_m$ must be minimal $(-b_{m,\min})$ and $b_r$ must be minimal (i.e., $-\min(b_{r,\min}, \eta_r p_{r,\max}/v)$), and $f = 0$.

The next step is to apply the Karush–Kuhn–Tucker (KKT) conditions on the augmented Hamiltonian in (14) (Bertsekas, 1999). This leads to the following stationary conditions:

$$\frac{\partial \overline{H}}{\partial f}(s, v, \lambda_1, \lambda_2, \mu, f) = \lambda_2 - v - \mu_1 - \mu_4 v = 0 \text{ if } f > 0, \ b_r = b_m = 0 \tag{18}$$

$$\frac{\partial \overline{H}}{\partial b_r}(s, v, \lambda_1, \lambda_2, \mu, b_r) = \lambda_2 - \eta v + \mu_2 + \mu_5 v = 0 \text{ if } b_r < 0, \ f = b_m = 0 \tag{19}$$

$$\frac{\partial \overline{H}}{\partial b_m}(s, v, \lambda_1, \lambda_2, \mu, b_m) = \lambda_2 + \mu_3 = 0 \text{ if } b_m < 0, b_r < 0, \ f = 0, \tag{20}$$

and they are undefined for $f = b_r = b_m = 0$. The second part of the KKT conditions consists of the complementary slackness conditions on the path constraints given by $\mu_i \geqslant 0, i = 1, \ldots, 7,$

$$\mu_1\left(f_{\max} - f\right) = 0, \mu_2\left(b_r + b_{r,\min}\right) = 0, \mu_3\left(b_m + b_{m,\min}\right) = 0, \mu_4\left(b_{\min} - \left(b_r + b_m\right)\right) = 0,$$
$$\mu_5\left(\eta_f p_{f,\max} - fv\right) = 0, \mu_6\left(\eta_r p_{r,\max} + b_r v\right) = 0, \mu_7\left(v_{\max} - v\right) = 0. \tag{21}$$

We can now describe the optimal driving regimes depending on the costate $\lambda_2$ by using PMP and the KKT conditions. The driving regimes are as follows:

1. **Maximum acceleration (MA).** For the first case $\lambda_2 > v$ holds with $f$ maximal ($f_{\max}(v(t))$). With (21) leading to the fact that $\mu_1 > 0$ or $\mu_5 > 0$ and, therefore, maximum traction is applied by $f = \min(f_{\max}, \eta_f p_{f,\max}/v)$. Condition (21) also indicates $\mu_2 = \mu_3 = \mu_4 = \mu_6 = 0$, since $b_r = b_m = 0$. Moreover, $\mu_7 = 0$, because the maximum speed $v_{\max}$ cannot be maintained during maximum acceleration.
2. **Cruising by partial traction (CR1).** The singular solution with $\lambda_2 = v$ and $f \in [0, f_{\max}(v(t))]$ holds for the second case. Again since $f > 0$, (18) and (21) dictates that $\mu_1 = \mu_2 = \mu_3 = \mu_4 = \mu_5 = \mu_6 = 0$. Furthermore, $\lambda_2(t) = v(t)$ holds for a nontrivial interval, and thus $\dot{\lambda}_2(t) = \dot{v}(t)$. Now (3) and (16) give $f - \lambda_1 + vr'(v) + \mu_7 = f - r(v) - g(s)$, which can be rewritten to

$$h(v) = -\lambda_1 + vr'(v) + \mu_7 + r(v) + g(s) = 0. \tag{22}$$

For a constant gradient, the function $h(v)$ is an increasing convex function with a unique solution $h(v_f) = 0$ for $v_f > 0$. For the case that $v_f < v_{max}$ resulting in $\mu_7 = 0$, we can rewrite Eq. (22) to

$$v_f r'(v_f) - \lambda_1 + r(v_f) + g(s) = 0, \tag{23}$$

which indicates that the speed $v_f$ depends on $\lambda_1$ and $g(s)$, since $r_0$, $r_1$ and $r_2$ are constants. Therefore, the speed has a unique solution $v_f$, i.e. cruising speed, when the gradient is constant. In the case $v = v_{max}$, then $\mu_6 = \lambda_1 - v_{max} r'(v_{max}) - r(v_{max}) - g(s)$. We also have $\dot{v}(t) = 0$ and thus the traction force is equal to the total resistance force in order to remain at the cruising speed, i.e. $f(t) = r(v_f) + g(s)$.

3. **Coasting (CO)**. The third case indicates that $\eta v < \lambda_2 < v$ and thus $f = b_r = b_m = 0$. The complementary slackness conditions (21) indicate that $\mu_1 = \mu_2 = \mu_3 = \mu_4 = \mu_5 = \mu_6 = 0$. Furthermore, the resistance influences the speed and, therefore, the speed limit can not be maintained, indicating that $\mu_7 = 0$.

4. **Cruising by partial regenerative braking (CR2)**. The fourth case is the second singular solution with $\lambda_2 = \eta v$ and $b_r \in [-\min(b_{r,min}, \eta_r p_{r,max}/v), 0]$ and $f = 0$, and $b_m = 0$, since $\lambda_2 > 0$. Since $b_r < 0$ the conditions (19) and (21) indicates that $\mu_1 = \mu_2 = \mu_3 = \mu_4 = \mu_5 = \mu_6 = 0$. Moreover, $\lambda_2(t) = \eta v(t)$ holds for a nontrivial interval, and thus $\dot{\lambda}_2(t) = \eta \dot{v}(t)$. Now (3) and (16) give $\eta b_r - \lambda_1 + \eta v r'(v) + \mu_7 = b_r - r(v) - g(s)$, which rewrites to

$$h(v) = -\lambda_1 + \eta v r'(v) + \mu_7 - (1-\eta) b_r + r(v) + g(s) = 0. \tag{24}$$

Like the driving regime CR1, we can prove that this equation results in a unique solution $v_r$ for constant gradient. The derivatives of $h(v)$ are $h'(v) = r'(v) + \eta r'(v) + \eta v r''(v) > 0$ and $h''(v) = r''(v) + 2\eta r''(v) + \eta v r'''(v) > 0$, which indicate that $h(v)$ is an increasing convex function with a unique solution $v_r$. For the condition $v_r < v_{max}$ and $\mu_7 = 0$, we can derive that the cruising speed must satisfy

$$\eta v_r r'(v_r) - \lambda_1 - (1-\eta) b_r + r(v_r) + g(s) = 0, \tag{25}$$

which indicates that $v_r$ depends on $\lambda_1$ and $g(s)$, since $r_0$, $r_1$ and $r_2$ are constants. Again, we find a constant cruising speed $v_r$ for constant gradients since we consider piecewise-constant gradients. In the case $v_r = v_{max}$, $\mu_7$ is defined by $\mu_7 = \lambda_1 + (1-\eta) b_r - r(v_{max}) - \eta v_{max} r'(v_{max}) - g(s)$. During cruising by partial regenerative braking, the regenerative braking force is equal to the total train resistance in order to remain at a constant cruising speed $v_b$, i.e. $b_r = r(v_r) + g(s)$, which indicates that this regime can only occur on negative slopes.

5. **Maximum regenerative braking (MRB)** The fifth case occurs if $0 < \lambda_2 < \eta v$ with $b_r$ minimal, i.e. $b_r = -\min(b_{r,min}, \eta_r p_{r,max}/v)$, and $f = 0$ and $b_m = 0$. From condition (19) follows that $\mu_2 > 0$, $\mu_6 > 0$, and $\mu_1 = \mu_3 = \mu_4 = \mu_5 = 0$. Moreover, the speed is below the speed limit, thus, $\mu_7 = 0$. If $v = v_{max}$, then the driving regime CR2 with maximum regenerative braking is applied.

6. **Cruising by maximum regenerative and partial mechanical braking (CR3)**. The sixth case is the third singular solution with $\lambda_2 = 0$ and $b_m \in [-b_{m,min}, 0]$, $b_r = -\min(b_{r,min}, \eta_r p_{r,max}/v)$ and $f = 0$. Since $b_m < 0$ and $b_r < 0$, the conditions (19), (20) and (21) indicate that $\mu_1 = \mu_3 = \mu_4 = \mu_5 = 0, \mu_2 > 0$ and $\mu_6 > 0$. Moreover, $\lambda_2(t) = 0$ holds for a nontrivial interval, and thus $\dot{\lambda}_2(t) = 0$. Now (16) gives

$$\lambda_1 = b_r(\eta - \mu_6) + \mu_7. \tag{26}$$

Moreover, we consider the maximized Hamiltonian (13) leading to:

$$H = (\lambda_1 - \eta b_r) v. \tag{27}$$

The maximized Hamiltonian is constant on sections with constant gradient. Furthermore, $\lambda_1$ is constant for $\lambda_2 = 0$ due to (15). The Hamiltonian is independent on $t$ and, therefore, the partial derivative to time is zero. Thus, (27) gives $\dot{\lambda}_1 v + (\lambda_1 - \eta b_r) \dot{v} = 0 + (\lambda_1 - \eta b_r)(b_r + b_m - r(v) - g(s)) = 0$. Then either the first factor must be zero or the second. In the first case, $\lambda_1 = \eta b_r$ and since $\lambda_1$ is a constant, so is $b_r$ and then by (27) also speed is constant. In the second case, $b_r + b_m - r(v) - g(s) = 0$ and then by (3) speed is constant and then so is $b_r$ by (27). In addition, (27) indicates that $v$ depends on $b_r$ which leads to a unique cruising speed $v_m$. If the speed is smaller than the speed limit ($v_m < v_{max}$), then $\mu_7 = 0$ and $\mu_6 = \eta - \lambda_1/b_r$ by (26) and else $\mu_7 > 0$, $\mu_6 \geqslant 0$ and $v_m = v_{max}$. During cruising with maximum regenerative and partial mechanical braking, the total braking force is equal to the total train resistance in order to remain at a constant cruising speed $v_m$, i.e. $b_m = r(v_m) + g(s) - b_r$, which indicates that this regime can only occur on negative slopes.

7. **Maximum braking (MB)** The seventh case is $\lambda_2 < 0$ with $b_m$ and $b_r$ minimal, and $f = 0$. From the stationary conditions (20) it follows that $\mu_2 = -\lambda_2 > 0$ and from (21) follows $\mu_3 > 0$, $\mu_4 > 0$, and $\mu_6 > 0$. Moreover, since $f = 0$ from (21) follows $\mu_1 = \mu_5 = 0$. Furthermore, if the speed is below the speed limit, then $\mu_7 = 0$. If $v = v_{max}$, then the sixth driving regime (CR3) with maximum total braking is applied bounded by (11).

The optimality conditions thus provide the following seven optimal driving regimes comparable to Baranov et al. (2011):

$$
\left(\widehat{f}(t), \widehat{b}_r(t), \widehat{b}_m(t)\right) = 
\begin{cases}
(f_{\max}(v(t)), 0, 0) & \text{if } \lambda_2(t) > v(t) & \text{(MA)} \\
(r(v(t)) + g(s), 0, 0) & \text{if } \lambda_2(t) = v(t) & \text{(CR1)} \\
(0, 0, 0) & \text{if } \eta v(t) < \lambda_2(t) < v(t) & \text{(CO)} \\
(0, r(v(t)) + g(s), 0) & \text{if } \lambda_2(t) = \eta v(t) & \text{(CR2)} \\
(0, -b_{r,\min}(v(t)), 0) & \text{if } 0 < \lambda_2(t) < \eta v(t) & \text{(MRB)} \\
(0, -b_{r,\min}(v(t)), r(v(t)) + g(s) - b_{r,\min}(v(t))) & \text{if } \lambda_2 = 0 & \text{(CR3)} \\
(0, -b_{r,\min}(v(t)), -(b_{\min} - b_{r,\min})) & \text{if } \lambda_2(t) < 0 & \text{(MB)},
\end{cases}
\tag{28}
$$

where $b_{r,\min}(v) = -\min(b_{r,\min}, \eta_r p_{r,\max}/v)$. The first driving regime is maximum acceleration (MA) in which the train applies the minimum of the maximum specific traction force $f_{\max}$ and the maximum specific traction power (including the traction efficiency $\eta_f$) divided by speed $\eta_f p_{f,\max}/v$. The train applies coasting (CO) by zero control, i.e., $f = b_r = b_m = 0$. The driving regime maximum regenerative braking (MRB) is applied to brake the train when the speed is below the optimal cruising speed, since then the train only uses the regenerative brakes in order to generate energy during braking. The maximum braking (MB) driving regime is used to brake as fast as possible and is used especially for low speeds, where regenerative braking does not generate (sufficient) energy or regenerative braking is not available (speeds close to zero). The other three driving regimes are cruising and all are singular solutions. If the solution satisfies $\lambda_2(t) = v(t)$ then the train is driving at a constant speed by using partial traction force in order to balance the total resistance (cruising partial traction, CR1). The second singular solution ($\lambda_2(t) = \eta v(t)$) is cruising by partial regenerative braking (CR2) in which the train applies the regenerative braking control in order to balance the total resistance, which might be needed at maximum speed with downhill slopes. The third singular solution ($\lambda_2 = 0$) consist of cruising by partial mechanical braking with maximum regenerative braking (CR3) in order to balance the total resistance. This holds for steep downhill slopes if regenerative braking alone is not sufficient to maintain the cruising speed. Note that the optimal control structure indicates that the mechanical braking control is only applied by the train in case that the regenerative braking control is insufficient to maintain an optimal cruising speed during steep downhill slopes (CR3) or during maximum braking (MB). The driving regimes with the switching points based on the costate $\lambda_2$ are the necessary optimality conditions. Algorithms like the pseudospectral method may be used to find the optimal sequence of the different driving regimes. In practice, energy-efficient train driving can be applied if the train is running on-time and the timetable provides sufficient running time supplements (Scheepmaker and Goverde, 2015). The general speed profile of the EETC RMeB driving strategy for a flat track without varying speed limits and sufficient running time supplements is shown in Fig. 2. Compared to mechanical braking only (see Section 2.3) or regenerative braking only (see Section 2.4), there are two different braking regimes consisting of maximum regenerative braking (MRB) and partial mechanical braking with maximum regenerative braking (CR3). In addition, we consider the nonlinear bounded regenerative braking behavior of the engine of the train.

### 2.3. Energy-efficient train control with constant-bounded regenerative braking only (RB)

In this section the EETC problem with just regenerative braking is discussed. Most research on EETC with regenerative braking considers no mechanical braking and just a constant maximal (regenerative) braking rate (Khmelnitsky, 2000; Franke et al., 2000; Albrecht et al., 2016a; Albrecht et al., 2016b; Scheepmaker et al., 2020). This is a special case of the optimal control problem discussed in Section 2.2, with $b_m = 0$, without the nonlinear regenerative braking constraint (5). Therefore, the objective function is equal to (1), subject to the constraints (2)–(4) and (6)–(11). It can be shown that this leads to the following optimal control structure:

$$
\left(\widehat{f}(t), \widehat{b}_r(t)\right) = 
\begin{cases}
(f_{\max}(v(t)), 0) & \text{if } \lambda_2(t) > v(t) & \text{(MA)} \\
(r(v(t)) + g(s), 0) & \text{if } \lambda_2(t) = v(t) & \text{(CR1)} \\
(0, 0) & \text{if } \eta v(t) < \lambda_2(t) < v(t) & \text{(CO)} \\
(0, r(v(t)) + g(s)) & \text{if } \lambda_2(t) = \eta v(t) & \text{(CR2)} \\
(0, -b_{r,\min}(v(t))) & \text{if } \lambda_2(t) < \eta v(t) & \text{(MRB)}.
\end{cases}
\tag{29}
$$
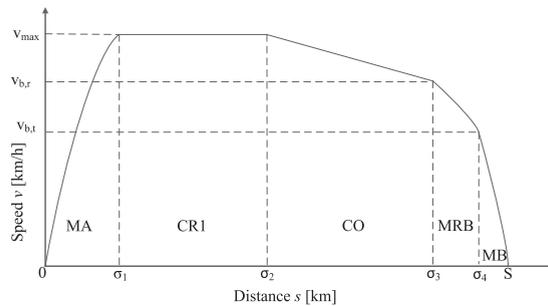


**Fig. 2.** Speed profile of a basic energy-efficient driving strategy with regenerative and mechanical braking including switching points between driving regimes at $\sigma_1, \sigma_2, \sigma_3,$ and $\sigma_4$ for a flat track without varying speed limits and sufficient running time supplements ($v_{\max}$ = optimal cruising speed, $v_{b,r}$ = speed at the start of the MRB regime, $v_{b,t}$ = speed at the start of the MB regime, MA = maximum acceleration, CR1 = cruising by partial traction, CO = coasting, MRB = maximum regenerative braking, and MB = maximum braking).

In this structure maximum braking (MRB) is achieved by applying the maximum regenerative braking force and cruising phase CR2 consists of partial regenerative braking. Therefore, the optimal driving regimes are similar to Section 2.2, with the only difference that the train applies only regenerative braking during the different braking regimes. Note that this driving strategy is normally not possible in practice, since the train needs to apply mechanical braking for speeds around zero in order to brake to standstill. However, we consider this driving strategy, since it is used in literature and so we want to compare the difference between EETC with both regenerative and mechanical braking to EETC with only regenerative braking. For a simple flat track without varying speed limits and sufficient running time supplements, the optimal driving strategy for regenerative braking only is visualized in Fig. 3 where now MB implies MRB as there is only one type of braking.

### 2.4. Energy-efficient train control with mechanical braking only (MeB)

In this section the EETC problem with only mechanical braking is discussed similar to for instance Howlett (2000) and Scheepmaker et al. (2020). The optimal control problem is again a special case of the one as discussed in Section 2.2, with $b_r = \eta = 0$. This leads to the following objective function:

$$E = \min \int_0^T f\left(t\right) v\left(t\right) dt, \tag{30}$$

subject to the constraints (2)–(11). This leads to the following optimal control structure:

$$\left(\widehat{f}(t), \widehat{b}_m(t)\right) = \begin{cases} (f_{\max}(v(t)), 0) & \text{if } \lambda_2(t) > v(t) & \text{(MA)} \\ (r(v(t)) + g(s), 0) & \text{if } \lambda_2(t) = v(t) & \text{(CR1)} \\ (0, 0) & \text{if } 0 < \lambda_2(t) < v(t) & \text{(CO)} \\ (0, r(v(t)) + g(s)) & \text{if } \lambda_2(t) = 0 & \text{(CR3)} \\ (0, -b_{m,\min}(v(t))) & \text{if } \lambda_2(t) < 0 & \text{(MB)}. \end{cases} \tag{31}$$

The regimes CR3 and MB are achieved by applying the mechanical brakes. Therefore, the optimal driving regimes are similar to Section 2.2, with the only difference that the train applies only mechanical during the different braking regimes. For a simple flat track without varying speed limits and sufficient running time supplements, the optimal driving strategy for mechanical braking only is visualized in Fig. 3. Note that this structure is the same as for regenerative braking only (during MB now mechanical braking is applied instead of regenerative braking).

### 2.5. Minimum-time train control

In this section the minimum-time train control (MTTC) problem is briefly discussed based on the problem formulation defined in Section 2.2. The aim of this problem is to minimize total running time of the train $t_f$ [s] which is free. The objective function $T$ [s] is given by

$$\text{Minimize } T = t_f - t_0, \tag{32}$$

subject to the constraints (2)–(11) and the endpoint conditions

$$t_0 = 0, v\left(t_0\right) = 0, v\left(t_f\right) = 0, s\left(t_0\right) = 0, s\left(t_f\right) = S. \tag{33}$$

Applying an analysis of the necessary optimality conditions similar to Section 2.2 leads to the following optimal control structure
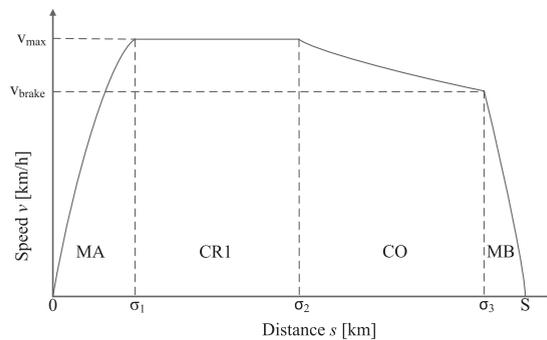


**Fig. 3.** Speed profile of a basic energy-efficient driving strategy with regenerative or mechanical braking only including switching points between driving regimes at $\sigma_1, \sigma_2$ and $\sigma_3$ for a flat track without varying speed limits and sufficient running time supplements (MA = maximum acceleration, CR1 = cruising by partial traction, CO = coasting, and MB = maximum braking).

$$\left(\widehat{f}(t),\widehat{b}(t)\right) = \begin{cases} (f_{\max}(v(t)),0) & \text{if } \lambda_2(t) > 0 & \text{(MA)} \\ (r(v_{\max}) + g(s),0) & \text{if } \lambda_2(t) = 0 \text{ and } r(v_{\max}) + g(s) \leqslant 0 & \text{(CR1)} \\ (0, r(v_{\max}) + g(s)) & \text{if } \lambda_2(t) = 0 \text{ and } r(v_{\max}) + g(s) > 0 & \text{(CR4)} \\ (0, -b_{\min}(v(t))) & \text{if } \lambda_2(t) < 0 & \text{(MB)}. \end{cases} \tag{34}$$

The results indicate a single singular solution (cruising) in which the train applies traction (CR1) or braking force (CR4) in order to remain at the speed limit, depending on the sign of the resistance. The train may apply cruising by partial braking during downhill slopes. The results show that the train accelerates and brakes as fast as possible and remains at the maximum speed in order to minimize the total running time. The optimal running strategy for a simple flat track without varying gradients is shown in Fig. 4.

In this case, we also have to consider the endpoint equations. The endpoint Lagrangian $\overline{E}$ [s] is

$$\overline{E}\left(s_f\left(t_f\right), v\left(t_f\right), t_f\right) = -t_f + \gamma_1\left(s\left(t_f\right) - S\right) + \gamma_2 v\left(t_f\right), \tag{35}$$

where $\gamma_1$ [s/m] and $\gamma_2$ [s$^2$/m] are Lagrange multipliers, with the complementary slackness conditions $\gamma_1(s(t_f) - S) = 0$ and $\gamma_2 v(t_f) = 0$. For the endpoint of the Hamiltonian we then have

$$\overline{H}\left(x_f\left(t_f\right), v\left(t_f\right), t_f\right) = -\frac{\partial \overline{E}}{\partial t_f} = 1. \tag{36}$$

Thus, the endpoint conditions indicate that the endpoint of the Hamiltonian $H$ is equal to one.

## 3. Pseudospectral method

In this paper the Radau Pseudospectral Method is applied in which orthogonal collocation at Legendre–Gauss-Radau (LGR) points is applied, which include the initial point. Details are given in of Rao et al. (2010) and Garg et al. (2009) and the transcription of the optimal train control problem to a discretized nonlinear programming problem is given in Goverde et al. (2020), Wang and Goverde (2016). There are different toolboxes available to solve the optimal control problem, like DIDO (Direct and Indirect Dynamic Optimization) (Ross and Karpenko, 2012; Ross, 2015), PSOPT (Becerra, 2010), and GPOPS (General Pseudospectral OPtimal Control Software) (Rao et al., 2010). We have chosen for GPOPS (Version 4.1) since this can be applied as a toolbox in MATLAB and evaluation of the costates and Hamiltonian value is possible, to validate whether the results are in line with optimal control theory. The resulting Hamiltonian $H$ and costate variable $\lambda_1$ should be constant when the gradient is constant.

We consider the multiple-phase pseudospectral method, where the trajectory consist of different phases. Each phase has its own cost function, dynamic, path and boundary constraints. The different phases are linked using linkage conditions and the total cost function is the sum of the individual cost functions of the different phases. Therefore, the total costs are minimized considering the different constraints within phases and the linkage conditions between phases. Within each phase we consider a constant speed limit and gradient, thus defining the phase boundaries. For the reference scenario without varying speed limits and gradients the model is reduced to the single-phase model. In this scenario we use a single-phase model with 200 collocation points, which was determined by trial-and-error and gave a good balance between the quality of the model results and the computation time. For the other scenarios we used the multiple-phase model where the number of collocation points and their distribution is determined by the algorithm of GPOPS.
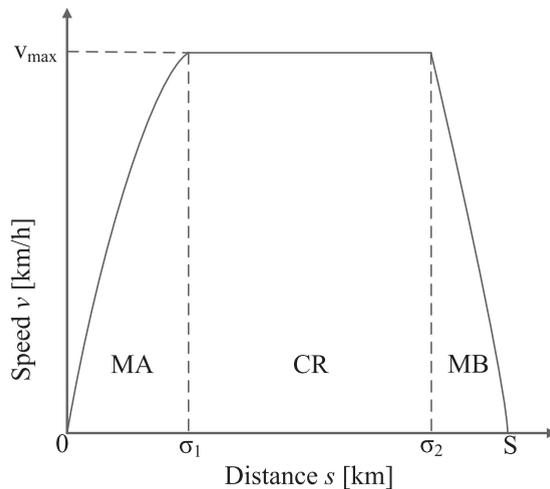
Fig. 4. Speed profile of a basic minimum time control strategy with switching points between driving regimes at $\sigma_1$ and $\sigma_2$ for a flat track without varying speed limits (MA = maximum acceleration, CR = cruising, and MB = maximum braking).

We refer to Wang and Goverde (2016) and Goverde et al. (2020) for the derivation of the multiple-phase optimal train control problem. For this paper, we extended the single-phase model developed by Scheepmaker and Goverde (2016) and Scheepmaker et al. (2020) to a multiple-phase model and we applied it on a laptop with a 2.1 GHz processor and 8 GB RAM.

We use a smoothing function based on a moving average over the control to correct for the numerical oscillations in the pseudospectral approximations during the singular solution of cruising (oscillation of the control). In GPOPS the discretized optimal control is approximated by alternating discrete values around the optimal value with the same objective value as the smooth (feasible) control.

## 4. Results

In this section we apply the multiple-phase pseudospectral model on different cases in order to investigate the effect of different braking strategies (i.e. mechanical and regenerative braking). We have also validated that the model results are in line with the necessary optimality conditions similar to Goverde et al. (2020). As illustration, we only show the validation process for the EETC-RMeB driving strategy in the reference scenario. We investigate different driving strategies. First, we have the minimum-time (MT) driving strategy, in which a train runs as fast as possible. Second, we consider the energy-efficient (EE) driving in which total traction energy consumption is minimized given the amount of running time supplements in the timetable. We investigate *combined nonlinear bounded regenerative and mechanical braking* (*RMeB*, see Section 2.2), *constant-bounded regenerative braking only* (*RB*, see Section 2.3) and *mechanical braking only* (*MeB*, see Section 2.4). Our main focus is to compare RMeB with MeB, but we also consider RB since this is used commonly in literature, e.g. Khmelnitsky (2000), Franke et al. (2000), and Albrecht et al. (2016a,b). Note that the difference between RMeB and RB is in the maximum braking rate. RMeB considers the regenerative and mechanical braking curve as shown in Fig. 5 with a nonlinear bounded regenerative braking limited by the maximum braking force. Note that in situations for RMeB where the maximum regenerative braking force is insufficient (i.e. driving regimes CR3 and MB in (28)) the train applies additional mechanical braking in order to overcome the gap between the requested braking force and the maximum regenerative braking force. RB uses a constant maximum regenerative braking rate.

We applied the model to a Dutch case study between the stations of Utrecht Central (Ut) and 's-Hertogenbosch (Ht). The total length of the section is 48.531 km. We only consider the double-deck rolling stock type VIRM-6, which is operated by the Netherlands Railways (NS). The static train parameters of the Intercity (IC) train are shown in Table 1 and Fig. 5. The specific parameters of (2)–(10), i.e., $p_{max}$, $f_{max}$, and $r(v)$, are computed by dividing the values of Table 1 by the total rotating mass. We assume that the accelerating train is similar to the regenerative braking train, which means that the traction efficiency for the regenerative braking train $\eta_f$ is the same as for the accelerating train $\eta_s$, i.e. $\eta_f = \eta_s = 87.5$ (see Table 1). Moreover, the traction efficiency of converting electricity into mechanical energy happens to be the same as converting mechanical energy into electricity in the rolling stock data of NS (2020). Therefore, $\eta_f = \eta_r = 87.5\%$ (see Table 1). We assume that the Dutch catenary efficiency for the 1.5 kV DC network is equal to $\eta_c = 80\%$ (Scheepmaker and Goverde, 2016). The efficiency of the catenary is used when we consider regenerative braking. In this scenario we consider the energy used by the second (accelerating) train. Therefore, we assume that the total efficiency for regenerative braking energy up to the traction energy for the accelerating train consists of $\eta = \eta_r \eta_c \eta_s = 0.6125$. After obtaining the relevant traction and braking forces, and speed over the trip by solving the optimal control problems as discussed in Section 2, PROMO computes the total energy consumption of the train $E$ [kWh] similar to Scheepmaker et al. (2020) at the catenary by using

$$E(t) = (P_e + P_c)t, \tag{37}$$

with the powers computed by
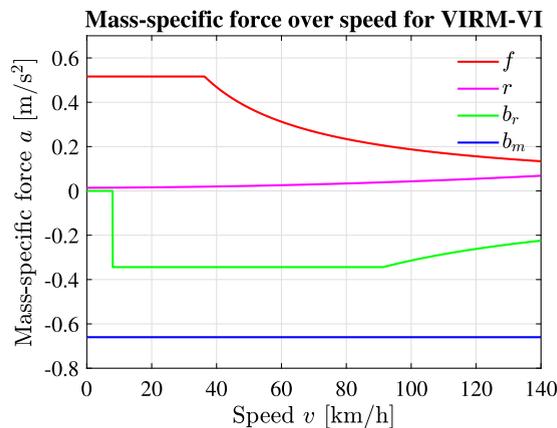


**Fig. 5.** Mass-specific force-speed diagram for VIRM-VI (*f*: mass-specific traction force, *r*: mass-specific train resistance, $b_r$: mass-specific regenerative braking force, and $b_m$: mass-specific mechanical braking force).

**Table 2**
Main results of the different scenarios.

| Scenario | Figure | Trip time (s) | RTS (%) | Energy consumption (kWh) | Energy saving (%) | Maximum speed (km/h) | $Q$ | $N$ | Costate variable $\lambda_1$ | Hamiltonian $H$ | Time (s) |
|---|---|---|---|---|---|---|---|---|---|---|---|
| Ref. IC MTTC-MeB | 7–9 | 1336 | 0 | 548.6 | 0 | 140.0 | 1 | 200 | 0.026 | 1.00 | 30.3 |
| Ref. IC MTTC-RB | 7–9 | 1336 | 0 | 496.9 | 9.4 | 140.0 | 1 | 200 | 0.026 | 1.00 | 30.7 |
| Ref.IC MTTC-RMeB | 7–9 | 1336 | 0 | 524.5 | 4.4 | 140.0 | 1 | 200 | 0.026 | 1.00 | 22.5 |
| Ref. IC EETC-MeB | 7–9 | 1537 | 15 | 394.5 | 28.1 | 126.1 | 1 | 200 | 0.141 | 2.88 | 40.3 |
| Ref. IC EETC-RB | 7–9 | 1537 | 15 | 376.9 | 31.3 | 122.5 | 1 | 200 | 0.114 | 2.63 | 91.2 |
| Ref. IC EETC-RMeB | 6–9 | 1537 | 15 | 380.8 | 30.6 | 123.2 | 1 | 200 | 0.136 | 2.69 | 42.3 |
| Ref. SPR MTTC-MeB | 11–13 | 450 | 0 | 219.7 | 0 | 140.0 | 1 | 200 | 0.026 | 1.00 | 39.3 |
| Ref. SPR MTTC-RB | 11–13 | 450 | 0 | 169.2 | 23.0 | 140.0 | 1 | 200 | 0.026 | 1.00 | 38.7 |
| Ref. SPR MTTC-RMeB | 11–13 | 450 | 0 | 196.1 | 10.8 | 140.0 | 1 | 200 | 0.026 | 1.00 | 38.9 |
| Ref. SPR EETC-MeB | 11–13 | 517 | 15 | 132.8 | 39.6 | 133.5 | 1 | 200 | 0.169 | 3.91 | 32.2 |
| Ref. SPR EETC-RB | 11–13 | 517 | 15 | 113.4 | 48.4 | 122.9 | 1 | 200 | 0.135 | 2.67 | 30.7 |
| Ref. SPR EETC-RMeB | 10–13 | 517 | 15 | 117.9 | 46.3 | 127.2 | 1 | 200 | 0.143 | 2.96 | 33.8 |
| R.l. case IC MTTC-MeB | 14–16 | 1618 | 0 | 420.2 | 0 | 140.0 | 78 | 4–12 | pwc | pwc | 164.0 |
| R.l. case IC MTTC-RB | 14–16 | 1618 | 0 | 288.2 | 31.4 | 140.0 | 78 | 4–12 | pwc | pwc | 279.0 |
| R.l. case IC MTTC-RMeB | 14–16 | 1618 | 0 | 337.3 | 19.7 | 140.0 | 78 | 4–12 | pwc | pwc | 255.2 |
| R.l. case IC EETC-MeB | 14–16 | 1780 | 10 | 242.8 | 42.2 | 129.5 | 78 | 4–12 | pwc | pwc | 408.9 |
| R.l. case IC EETC-RB | 14–16 | 1780 | 10 | 204.1 | 51.4 | 123.5 | 78 | 4–12 | pwc | pwc | 545.6 |
| R.l. case IC EETC-RMeB | 14–16 | 1780 | 10 | 207.6 | 50.6 | 124.1 | 78 | 4–12 | pwc | pwc | 465.6 |
| R.l. case SPR MTTC-MeB | 17–19 | 545 | 0 | 150.9 | 0 | 130.0 | 38 | 4–12 | pwc | pwc | 20.0 |
| R.l. case SPR MTTC-RB | 17–19 | 545 | 0 | 103.8 | 31.2 | 130.0 | 38 | 4–12 | pwc | pwc | 28.4 |
| R.l. case SPR MTTC-RMeB | 17–19 | 545 | 0 | 126.6 | 16.1 | 130.0 | 38 | 4–12 | pwc | pwc | 24.7 |
| R.l. case SPR EETC-MeB | 17–19 | 599 | 10 | 89.5 | 40.7 | 121.6 | 38 | 4–12 | pwc | pwc | 53.1 |
| R.l. case SPR EETC-RB | 17–19 | 599 | 10 | 62.5 | 58.6 | 121.0 | 38 | 4–12 | pwc | pwc | 75.7 |
| R.l. case SPR EETC-RMeB | 17–19 | 599 | 10 | 67.2 | 55.5 | 123.0 | 38 | 4–12 | pwc | pwc | 56.8 |

Legend: RTS = running time supplements, $Q$ = Number of phases, $N$ = Number of collocation points per phase, pwc = piecewise constant, IC = Intercity, SPR = Sprinter, MTTC = Minimum Time Train Control, EETC = Energy-Efficient Train Control, MeB = Mechanical Braking, RB = constant-bounded Regenerative Braking, RMeB = nonlinear bounded Regenerative and Mechanical Braking, Ref. = reference, R.l. = real-life.

$$P_e = \left(\frac{F}{\eta_f} + B_r\eta\right)v \text{ and } P_c = \left(\frac{P_e}{V}\right)^2 W, \tag{38}$$

where $P_e$ [kW] is the traction power of the train, $P_c$ [kW] is the power over the catenary, $V$ [V] is the voltage, and $W$ [$\Omega$] is the resistance. In addition, we assumed that the average voltage over the catenary is $V = 1500$ V and the average resistance over catenary and tracks is $W = 0.1136$ $\Omega$ (Scheepmaker et al., 2020). We also consider the regenerative braking power of the train $P_r$ [kW] that limits the maximum regenerative braking force for the hyperbolic part in Fig. 1, which is provided by the rolling stock data (NS, 2020).

We consider different scenarios in order to investigate if the model results of the multiple-phase model are in line with the necessary optimality conditions as discussed in Section 2. We begin with the reference case without any varying speed limits and gradients with 15% of running time supplements for the EE driving strategy by using the single-phase model. In this section we also compare the driving strategy RMeB with RB. We consider a long train run (Intercity train run between Ut and Ht) as well as a short train run (Sprinter (SPR) train run between Zaltbommel (Zbm) and Ht). Afterwards, we consider the real-life case for both the IC and SPR train run with the actual speed limit and gradients of the corridor Ut-Ht, also with rolling stock type VIRM-6 for the multiple-phase model. In total we consider four different scenarios, see Table 2.

### 4.1. Reference scenario

In this subsection the results of the reference scenario are discussed. We start with a non-stop Intercity train service between Ut and Ht (about 48.5 km) in Section 4.1.1. In Section 4.1.2 we consider a train run of a Sprinter train between the stops Zbm and Ht (about 14 km). Finally, Section 4.1.3 gives a summary of the reference scenario.

### 4.1.1. Intercity train

The results of the different driving strategies can be found in Figs. 6–9 and Table 2. The results of the EETC-RMeB driving strategy are in line with the necessary optimality conditions. First, Table 2 shows that the costate $\lambda_1$ and Hamiltonian $H$ remain constant, since the gradient is constant as stated in (15). Second, the relation between costate $\lambda_2$ and speed $v$ is clearly visible in Fig. 6 representing the necessary optimality conditions given by (28). We see that the train applies maximum acceleration (MA) if $\lambda_2 > v$. Afterwards, cruising (CR1) is applied if $\lambda_2 = v$, followed by coasting (CO) if $\eta v < \lambda_2 < v$. After CO the train starts to apply maximum regenerative braking (MRB) for $0 < \lambda_2 < \eta v$, followed by maximum braking (MB) with combined mechanical and regenerative braking when $\lambda_2 < 0$. Note that cruising by partial braking does not occur, because there are no downward gradients in this scenario.

The energy consumption of MTTC-MeB is about 549 kWh. The difference between combined regenerative and mechanical braking with mechanical braking only is about 4.4%, and the difference between regenerative braking only versus mechanical braking only is about 9.4% in energy savings. This indicates that the unrealistic MTTC-RB overestimates the energy savings by 5 percent points. The structure of the optimal driving strategy is exactly the same, since the aim is to minimize total travel time. The model results are all generated in about 30 s.

The driving strategy of EETC-RMeB differs from both EETC-RB and EETC-MeB. The main difference betweeen EETC-RMeB and EETC-RB is that RB leads to a an overestimation of the energy savings of 1.0% by the unrealistic assumption of regenerative braking only at a constant braking rate. The RMeB driving strategy includes an extra maximum regenerative braking phase besides the maximum braking (see Fig. 8 and Fig. 9) starting below 83 km/h with a deceleration rate of 0.34 m/s². Therefore, the train applies a higher cruising speed as well as a shorter coasting phase for RMeB compared to RB and, thus, the results of RMeB show a clear balance
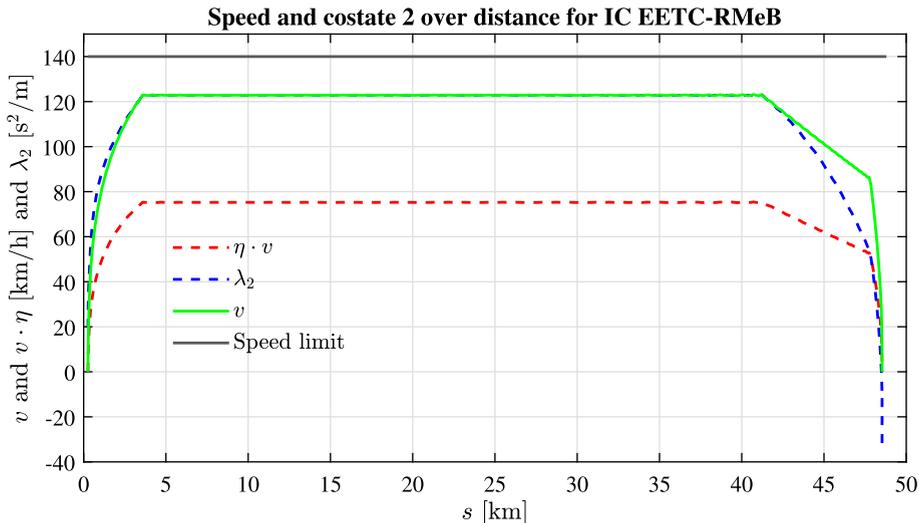


**Fig. 6.** Validation of the reference scenario for the IC with the EETC-RMeB driving strategy by using the speed/costate $\lambda_2$-distance profile.
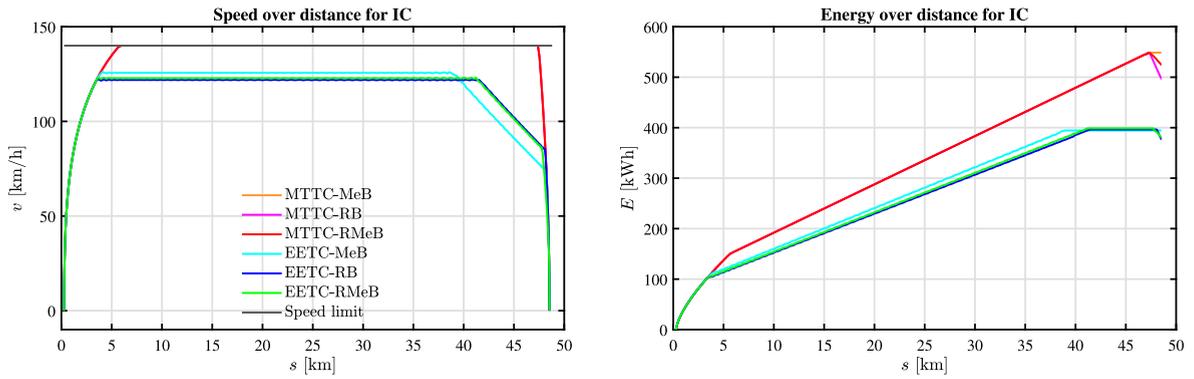
**Fig. 7.** Reference scenario for the IC with the speed-distance profile (left) and energy-distance profile of the different driving strategies (right).
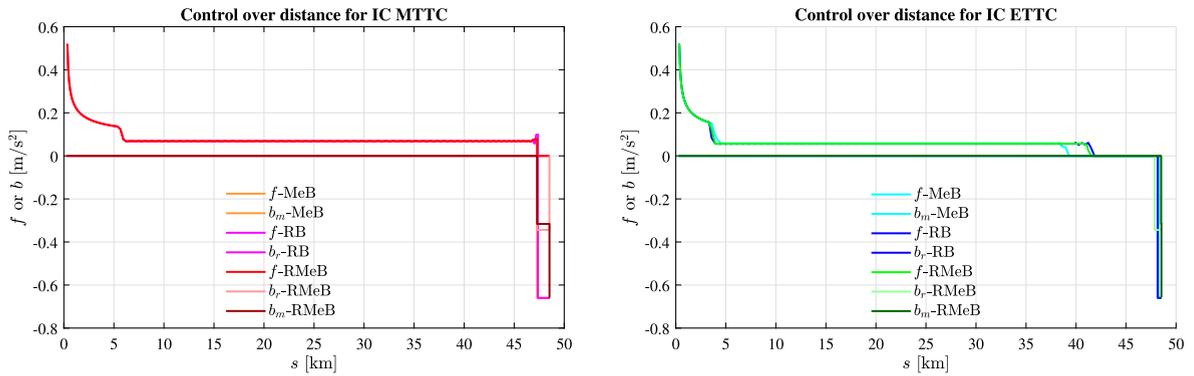


**Fig. 8.** Reference scenario for the IC with the control-distance profile for the MTTC (left) and EETC (right) driving strategies.
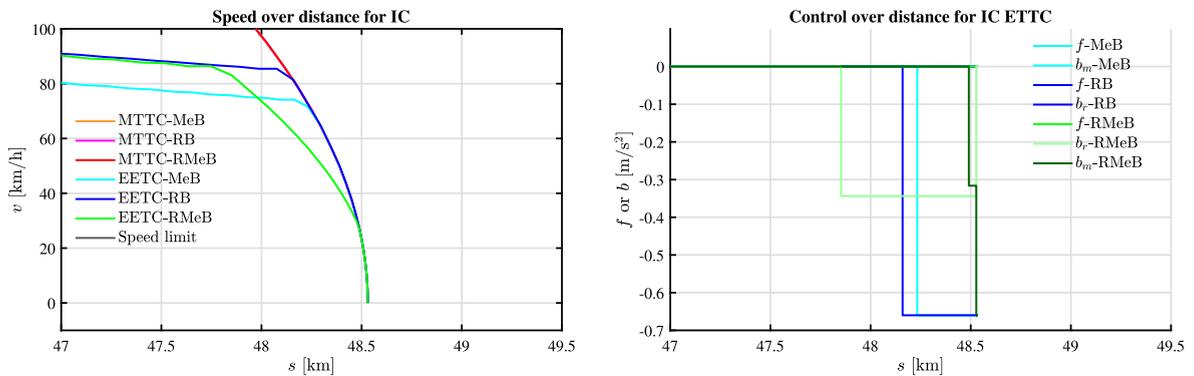


**Fig. 9.** Reference scenario for the IC zoomed in for the braking behavior of the energy-efficient driving strategies with the speed-distance profile (left) and control-distance profile (right).

between the train applying coasting in order to save energy and regenerative braking in order to regenerate energy. Only at speeds below 27 km/h maximum braking (including mechanical braking) is applied at a deceleration rate of 0.66 m/s$^2$. Based on the output of the model we computed that the energy saving by regenerative braking in the maximum braking driving regime is 0.3% (1.1 kWh) compared to the total energy consumption. The time the train applies regenerative braking during the maximum braking regime is about 8 s. Therefore, for the EETC-RMeB driving strategy more energy saving can be achieved by coasting than by applying regenerative braking at speeds below 27 km/h. The energy savings of EETC-MeB, EETC-RB, and EETC-RMeB compared to MTTC-MeB are about 28.1%, 31.3%, and 30.6%. Finally, the model results of EETC-MeB, EETC-RB, and EETC-RMeB are generated within 41 s, 92 s, and 43 s.

#### 4.1.2. Sprinter train

Figs. 10–13 and Table 2 show the results of the different driving strategies for the Sprinter train. Table 2 indicates that costate $\lambda_1$ remains constant due to the constant gradient as stated by (15). Costate $\lambda_2$ also behaves according to the necessary conditions given in (28) as can be seen in Fig. 10, $\lambda_2 > v$ during the driving regime MA, $\lambda_2 = v$ during cruising (CR1), $\eta v < \lambda_2 < v$ during CO, $0 < \lambda_2 < \eta v$ during RMB, and $\lambda_2 < 0$ during MB. The Hamiltonian remains constant. The MTTC-MeB driving strategy uses about 220 kWh. The MTTC-RMeB leads to energy savings of about 11% compared to MTTC-MeB. MTTC-RB leads to the unrealistic highest savings of 23%. The results are generated in 40 s (MTTC-MeB), 39 s (MTTC-RB), and 39 s (MTTC-RMeB).

The results of the shorter train route for the EE driving strategies indicates a clear difference in the optimal speed profile for the different braking strategies. EETC-RMeB and EETC-RB driving strategy have a short cruising phase, which is not included for the EETC-MeB driving strategy. In addition, the coasting phase is shorter for both regenerative braking strategies compared to EETC-MeB, which leads to a higher speed at the beginning of the braking phase. The difference between EETC-RB and EETC-RMeB is that the cruising speed for EETC-RMeB is higher, the coasting phase is shorter and the speed at the beginning of the braking phase is higher. In addition, the EETC-RMeB includes a phase of maximum regenerative braking only at speeds below 89 km/h with a deceleration rate of 0.34 m/s$^2$, and at speeds below 32 km/h the train applies maximum braking at 0.66 m/s$^2$ including mechanical braking. Note that below $v_1 = 8$ km/h maximum braking is applied by mechanical braking only, see Table 1. Like the Intercity train in Section 4.1.1 the results of the Sprinter train indicate that it is more efficient to start coasting earlier instead of applying regenerative braking only at speeds below 32 km/h.

The EETC-MeB leads to a energy saving of 39.6% compared to MTTC-MeB. EETC-RMeB increases the energy savings by 11.2% compared to EETC-MeB (46.3% energy savings compared to MTTC-MeB). EETC-RB would save up to 48.4% energy. The computation time of the EE driving strategies are about 32 s (EETC-MeB), 31 s (EETC-RB), and 34 s (EETC-RMeB).

#### 4.1.3. Summary reference scenario

When using regenerative braking (RMeB or RB) for the IC trip the cruising speed is lower, the cruising phase is longer, the coasting phase is shorter and the start of the braking speed is higher compared to pure mechanical braking. For the shorter train route (SPR), regenerative braking leads to a cruising phase, while mechanical braking directly starts to coast after maximum acceleration. The main difference between the driving strategies RMeB and RB for both the long and short trips is that RMeB has a higher cruising speed, a shorter coasting phase and an extra braking phase (maximum regenerative braking) compared to RB, which indicates a balance between coasting and regenerative braking, and mechanical braking is only used for maximum braking. RB overestimates the energy savings compared to RMeB. The results also indicate that the relative energy savings are higher for the shorter trip compared to the longer trip, since the coasting phase is relatively large compared to the other driving regimes.

### 4.2. Real-life case scenario

In this subsection we apply our model on a real-life case study for the train route between Utrecht Central and 's-Hertogenbosch in the Netherlands. We consider 10% running time supplements for the energy-efficient driving strategy. We start with the IC trip of about 48.5 km (Ut-Ht) in Section 4.2.1 followed by the SPR trip of about 14 km (Zbm-Ht) in Section 4.2.2. Finally, the summary of the case scenario is provided in Section 4.2.3.
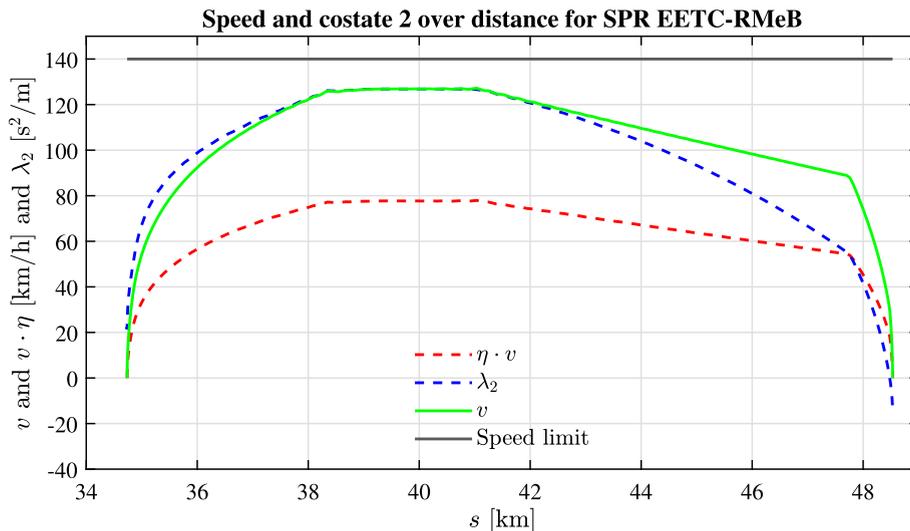


**Fig. 10.** Validation of the reference scenario for the SPR with the EETC-RMeB driving strategy by using the speed/costate $\lambda_2$-distance profile.
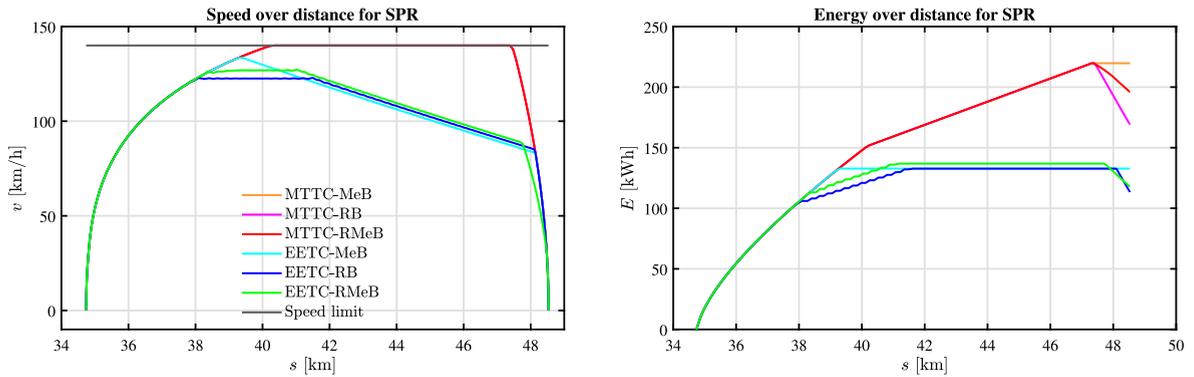
**Fig. 11.** Reference scenario for the SPR with the speed-distance profile (left) and energy-distance profile of the different driving strategies (right).
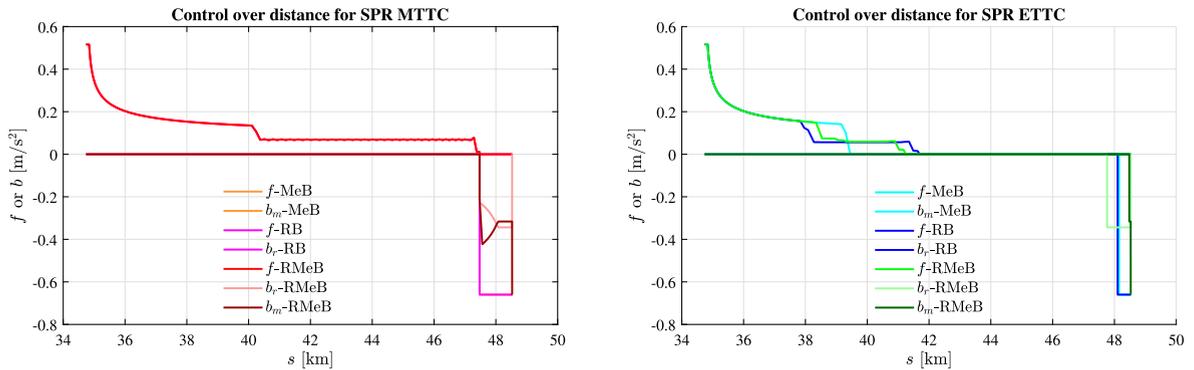


**Fig. 12.** Reference scenario for the SPR with the control-distance profile for the MTTC (left) and EETC (right) driving strategies.
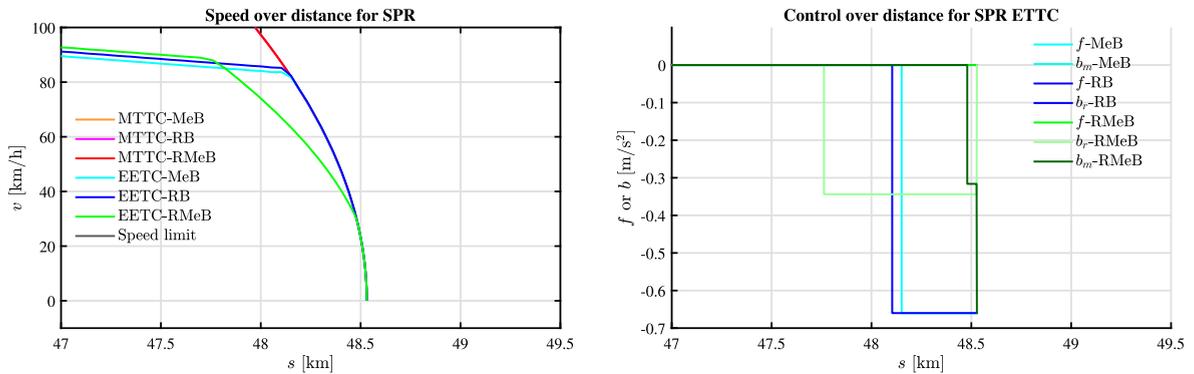


**Fig. 13.** Reference scenario for the SPR zoomed in for braking behavior of the energy-efficient driving strategies with the speed-distance profile (left) and control-distance profile (right).

#### 4.2.1. Intercity train route

The results of the different driving regimes are shown in Figs. 14–16 and Table 2. The energy consumption of MTTC-MeB is about 420 kWh. MTTC-RMeB can lead up to 19.7% extra energy savings. MTTC-RB would lead to extra energy savings of 14.6% compared to MTTC-RMeB. The computation time of the algorithm is about 164 s for the MTTC-MeB driving strategy, 279 s for the MTTC-RB driving strategy, and 255 s for the MTTC-RMeB driving strategy.

The speed profile of EETC-RMeB differs from EETC-MeB, see Fig. 14 for the complete trajectory and Fig. 16 showed specific details for the braking driving regimes by zooming in. The main differences are that the cruising speed is lower, the coasting phase is shorter and the speed at the beginning of the braking phase is higher. The difference between the EETC-RMeB and EETC-RB driving strategy is quite small. The main differences occur during braking as can be seen in the control-distance plots in Fig. 15. The RMeB driving strategy includes a phase of pure regenerative braking (RMB driving regime) and only at the final braking stage mechanical braking is
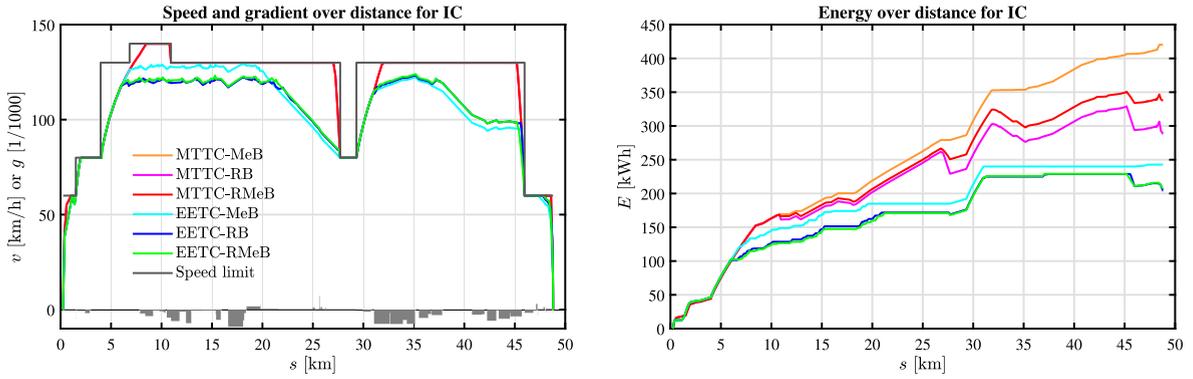
**Fig. 14.** Real-life case scenario for the IC (Ut-Ht) with the speed/gradient-distance profile (left) and energy-distance profile of the different driving strategies (right). The grey area in the left figure indicates the gradients [‰].
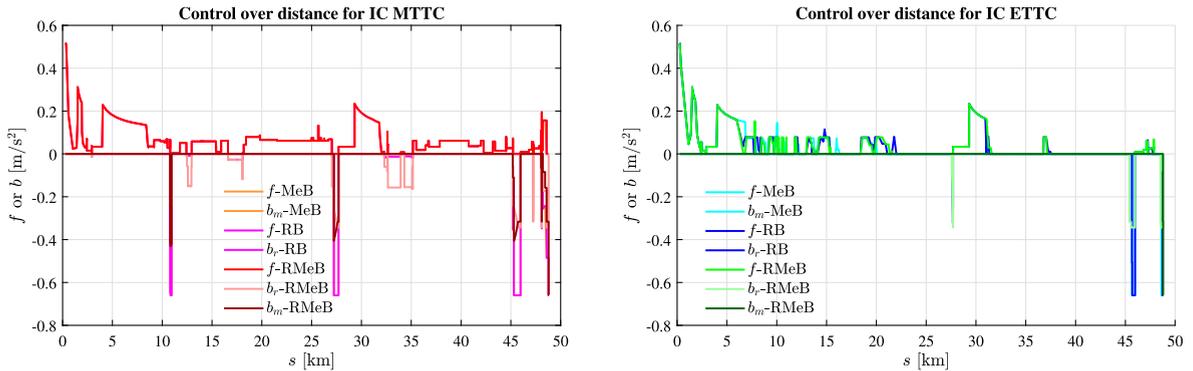


**Fig. 15.** Real-life case scenario for the IC (Ut-Ht) with the control-distance profile for the MTTC (left) and EETC (right) driving strategies.
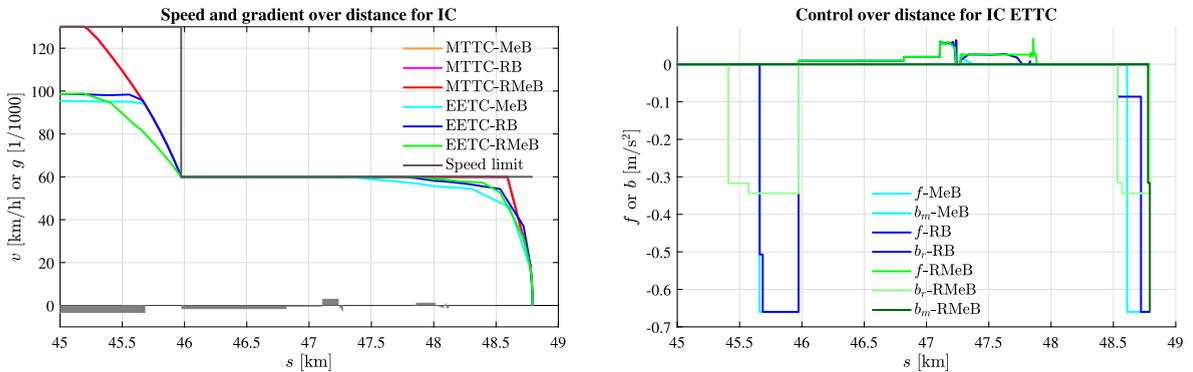


**Fig. 16.** Real-life case scenario for the IC (Ut-Ht) zoomed in between 45 km and 49 km for the braking behavior of the energy-efficient driving strategies with the speed/gradient-distance profile (left) and control-distance profile (right). The grey area in the left figure indicates the gradients [‰].

added to apply maximum braking (MB) for speeds below 20 km/h. The speed and control plots indicate that the train starts to brake earlier with the EETC-RMeB driving strategy compared to the other EE driving strategies. The EETC-MeB driving strategy leads to energy savings of 42.2% compared to MTTC-MeB, and EETC-RMeB can save even 14.5% more energy compared to EETC-MeB (50.6% compared to MTTC-MeB). EETC-RB would lead to the highest energy savings compared to MTTC-MeB of 51.4%. The computation time of EETC-MeB is about 409 s, EETC-RB is about 546 s, and EETC-RMeB takes about 466 s.

### 4.2.2. Sprinter train route

We apply the model also for a Sprinter route between Zaltbommel and 's-Hertogenbosch with the same IC rolling stock. The results

of the different driving strategy can be found in Figs. 17–19 and Table 2. The energy consumption of MTTC-MeB is about 151 kWh. The MTTC-RMeB driving strategy can save up to 16.1% compared to MTTC-MeB driving strategy, while the MTTC-RB driving strategy can save 31.2% compared to the MTTC-MeB driving straregy. The computation time of the model is 20 s for MTTC-MeB, 28 s for MTTC-RB, and 25 s for MTTC-RMeB.

The energy savings of EETC-MeB are about 40.7% compared to MTTC-MeB. EETC-RMeB can even lead to 55.5% savings compared to MTTC-MeB. EETC-RB would reach energy savings of even 58.6% compared to MTTC-MeB. The biggest difference in the EE driving strategies is between mechanical braking and the other braking strategies. EETC-RMeB accelerates to a higher maximum speed, has a shorter coasting phase and a regenerative braking phase, while mechanical braking is only added at speeds below 25 km/h, see the complete trajectory in Fig. 17 and Fig. 18, and for the details of the different braking regimes (by zooming in) see Fig. 19. The control-distance plots in Fig. 18 and Fig. 19 clearly indicate that the EETC-RMeB driving strategy starts the earliest with the braking around 45 km, while the other EE driving strategies starts by applying maximum braking around 45.5 km. The same observations of the difference in braking behavior can be seen around 48.5 km.

Again the resulting speed profiles of EETC-MeB and EETC-RMeB are different, due to the different braking behavior since during braking. EETC-RMeB saves relatively a large amount of energy by regenerative braking compared to the total energy of the trip. During the downhill sections in the coasting phase, the train maintains its speed. In addition, the EETC-MeB and EETC-RB speed profile are almost equal, except at the end of the trip (around 47.5 km) where EETC-MeB is focused on coasting while EETC-RB is focused on both coasting and regenerative braking. The computation time of EETC-MeB is about 53 s, EETC-RB is about 76 s, and EETC-RMeB takes about 57 s.

### 4.2.3. Summary real-life case

The application of the different driving strategies in the two real-life cases shows that the braking behavior does influence the structure of the optimal speed profile. In general, the EETC-RB driving strategy leads to the highest energy savings, followed by EETC-RMeB, because during braking energy is regenerated. For the IC case the EETC-RMeB and EETC-RB speed profile are different compared to the EETC-MeB driving strategy. Including (partly) regenerative braking in the EE driving strategy leads to a lower optimal cruising speed, shorter coasting and a higher speed at the beginning of the braking phase. EETC-RMeB applies an earlier braking compared to EETC-RB and only uses maximum braking at the end of the trip (braking for standstill). For the SPR case the driving regime of EETC-RMeB is different compared to EETC-MeB and EETC-RB (EETC-MeB and EETC-RB are quite similar). EETC-RMeB has a higher maximum speed, a shorter coasting phase and a higher speed at the beginning of the braking phase compared to the other EE driving strategies. Finally, the shorter distance scenario (SPR) between stops indicates relatively higher energy savings by the EE driving strategies compared to the longer distance IC scenario, because the coasting phase is a significant part of the total driving strategy. The findings of the real-life case are consistent with the general findings of the reference case.

## 5. Conclusion

This paper investigated the difference between mechanical and regenerative braking on the energy-efficient driving strategy using a multiple-phase pseudospectral optimal train control method for a single train. We model regenerative braking using the physical nonlinear bounded braking-speed functional relation, which could be supported by mechanical braking when needed, and compare this with pure mechanical braking and pure constant-bounded regenerative braking as is common applied in the literature. We derived the necessary optimality conditions for the energy-efficient driving strategy with mechanical and/or regenerative braking. The optimal control problems were solved using the multiple-phase pseudospectral method. We applied the models on different scenarios where we investigated the effect of the varying speed limit and gradients on the driving strategies.

The main differences between regenerative braking and pure mechanical braking for the EE driving strategies are that regenerative braking EE driving strategies apply a lower optimal cruising speed and have a higher speed at the beginning of the braking phase. For
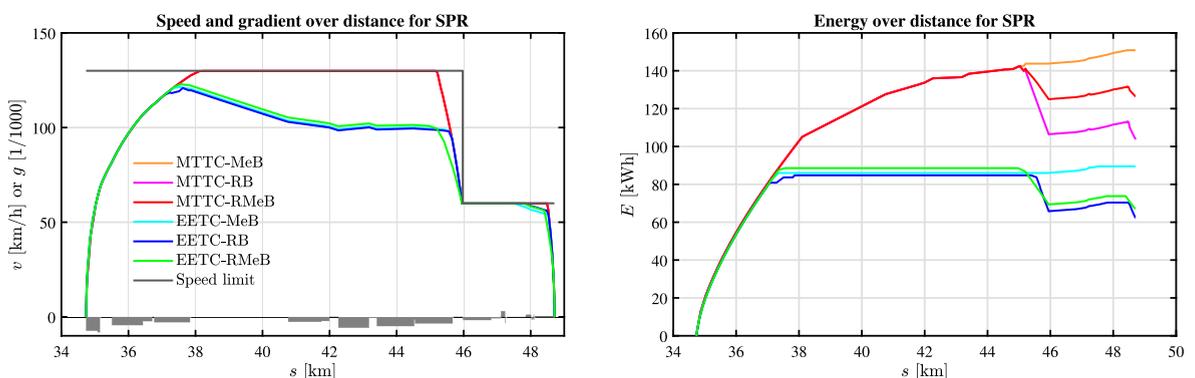


**Fig. 17.** Real-life case scenario for the SPR (Zbm-Ht) with the speed/gradient-distance profile (left) and energy-distance profile of the different driving strategies (right). The grey area in the left figure indicates the gradients [‰].
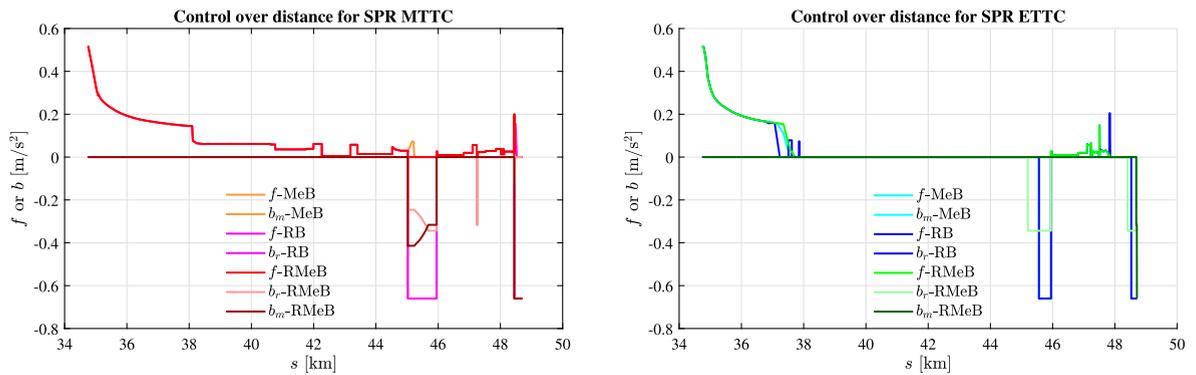
**Fig. 18.** Real-life case scenario for the SPR (Zbm-Ht) with the control-distance profile for the MTTC (left) and EETC (right) driving strategies.
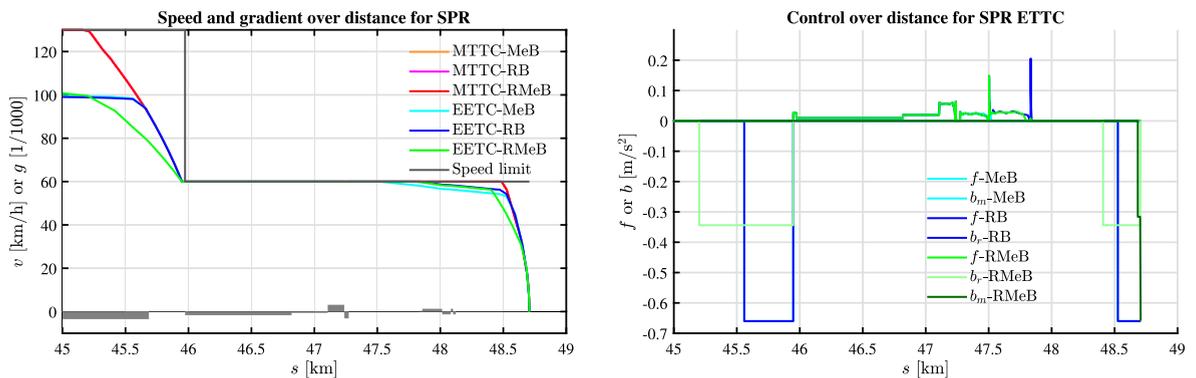


**Fig. 19.** Real-life case scenario for the SPR (Zbm-Ht) zoomed in between 45 km and 49 km for the braking behavior of the energy-efficient driving strategies with the speed/gradient-distance profile (left) and control-distance profile (right). The grey area in the left figure indicates the gradients [‰].

shorter distances EETC-MeB does not have a cruising phase, while EETC-RMeB and EETC-RB do have a cruising phase. The main difference between EETC-RMeB and EETC-RB is that the EETC-RMeB driving strategy considers the nonlinear bounded regenerative braking force diagram with possible additional mechanical braking in order to compensate regenerative braking (for example at low speeds), while EETC-RB considers only a constant regenerative braking. This leads to a higher cruising speed, a shorter coasting phase and a longer braking phase for EETC-RMeB. Therefore, current literature that focused on a constant regenerative braking rate over-estimates the energy savings gained by regenerative braking and does not compute to the optimal trajectory in practice for regenerative braking trains. Finally, the relative energy savings for the EE driving strategies are higher for shorter distances, because coasting is relatively the longest driving regime for short train routes and cruising becomes more significant for the longer train routes. Future research on regenerative braking for EETC will focus on the interaction with the neighboring trains including factors such as the driving strategy of the surrounding train, the distance between the synchronizing trains and the maximum allowable voltage of the power supply system.

## CRediT authorship contribution statement

**Gerben M. Scheepmaker:** Conceptualization, Methodology, Formal analysis, Investigation, Data curation, Software, Validation, Writing - original draft, Writing - review & editing. **Rob M.P. Goverde:** Conceptualization, Methodology, Formal analysis, Writing - review & editing, Resources, Supervision.

## Acknowledgements

## References

Albrecht, A.R., Howlett, P.G., Pudney, P.J., Vu, X., Zhou, P., 2016a. The key principles of optimal train control-part 1: Formulation of the model, strategies of optimal type, evolutionary lines, location of optimal switching points. Transport. Res. Part B: Methodol. 94, 482–508.

Albrecht, A.R., Howlett, P.G., Pudney, P.J., Vu, X., Zhou, P., 2016b. The key principles of optimal train control-part 2: Existence of an optimal strategy, the local energy minimization principle, uniqueness, computational techniques. Transport. Res. Part B: Methodol. 94, 509–538.

Albrecht, T., 2004. Reducing power peaks and energy consumption in rail transit systems by simultaneous train running time control. In: Allen, J., Brebbia, A., Hill, R. J., Sciutto, G., Sone, S. (Eds.), Computers in Railways IX. WIT Press, Southampton, UK, pp. 885–894.

Asnis, I.A., Dmitruk, A.V., Osmolovskii, N.P., 1985. Solution of the problem of the energetically optimal control of the motion of a train by the maximum principle. USSR Comput. Math. Math. Phys. 25 (6), 37–44.

Baranov, L.A., Meleshin, I.S., Chin', L.M., 2011. Optimal control of a subway train with regard to the criteria of minimum energy consumption. Russ, Electr. Eng. 82 (8), 405–410.

Becerra, V.M., 2010. Solving complex optimal control problems at no cost with psopt. In: 2010 IEEE International Symposium on Computer-Aided Control System Design, pp. 1391–1396.

Bertsekas, D.P., 1999. Nonlinear Programming. Athena Scientific, Belmont, MA, USA.

Brünger, O., Dahlhaus, E., 2014. Running time estimation. In: Hansen, I.A., Pachl, J. (Eds.), Railway Timetabling & Operations. Eurailpress, Hamburg, Germany, pp. 65–89.

Davis, W., 1926. The tractive resistance of electric locomotives and cars. General Electr. Rev. 29.

Fernández-Rodríguez, A., Fernández-Cardador, A., Cucala, A.P., 2018. Real time eco-driving of high speed trains by simulation-based dynamic multi-objective optimization. Simul. Model. Pract. Theory 84, 50–68.

Franke, R., Terwiesch, P., Meyer, M., 2000. An algorithm for the optimal control of the driving of trains. In: Proceedings of the 39th IEEE Conference on Decision and Control. Vol. 3. pp. 2123–2128.

Frilli, A., Meli, E., Nocciolini, D., Pugi, L., Rindi, A., 2016. Energetic optimization of regenerative braking for high speed railway systems. Energy Convers. Manage. 129, 200–215.

Garg, D., Patterson, M.A., Hager, W.W., Rao, A.V., Benson, D.A., Huntington, G.T., 2009. An overview of three pseudospectral methods for the numerical solution of optimal control problems. Adv. Astronaut. Sci. 135 (1), 475–487.

Ghaviha, N., Bohlin, M., Holmberg, C., Dahlquist, E., 2019. Speed profile optimization of catenary-free electric trains with lithium-ion batteries. J. Modern Transport. 27 (3), 153–168.

Ghaviha, N., Bohlin, M., Holmberg, C., Dahlquist, E., Skoglund, R., Jonasson, D., 2017. A driver advisory system with dynamic losses for passenger electric multiple units. Transport. Res. Part C: Emerg. Technol. 85, 111–130.

González-Gil, A., Palacin, R., Batty, P., 2013. Sustainable urban rail systems: Strategies and technologies for optimal management of regenerative braking energy. Energy Convers. Manage. 75, 374–388.

González-Gil, A., Palacin, R., Batty, P., Powell, J.P., 2014. A systems approach to reduce urban rail energy consumption. Energy Convers. Manage. 80, 509–524.

Goverde M.P., Rob, Scheepmaker M., Gerben, Wang, Pengling, 2020. Pseudospectral optimal train control. Europ. J. Operat. Res. https://doi.org/10.1016/j.ejor.2020.10.018.

Howlett, P.G., 2000. The optimal control of a train. Ann. Oper. Res. 98 (1), 65–87.

Howlett, P.G., Pudney, P.J., 1995. Energy-Efficient Train Control. Springer, London, UK.

Khmelnitsky, E., 2000. On an optimal control problem of train operation. IEEE Trans. Autom. Control 45 (7), 1257–1266.

Lewis, F.L., Vrabie, D.L., Syrmos, V.L., 2012. Optimal Control. John Wiley & Sons, Hoboken, NJ, USA.

Li, X., Lo, H.K., 2014a. An energy-efficient scheduling and speed control approach for metro rail operations. Transport. Res. Part B: Methodol. 64, 73–89.

Li, X., Lo, H.K., 2014b. Energy minimization in dynamic train scheduling and control for metro rail operations. Transport. Res. Part B: Methodol. 70, 269–284.

Liu, R.R., Golovitcher, I.M., 2003. Energy-efficient operation of rail vehicles. Transport. Res. Part A: Policy Pract. 37 (10), 917–932.

Lu, S., Weston, P., Hillmansen, S., Gooi, H.B., Roberts, C., 2014. Increasing the regenerative braking energy for railway vehicles. IEEE Trans. Intell. Transp. Syst. 15 (6), 2506–2515.

Luan, X., Wang, Y., De Schutter, B., Meng, L., Lodewijks, G., Corman, F., 2018a. Integration of real-time traffic management and train control for rail networks - part 1: Optimization problems and solution approaches. Transport. Res. Part B: Methodol. 115, 41–71.

Luan, X., Wang, Y., De Schutter, B., Meng, L., Lodewijks, G., Corman, F., 2018b. Integration of real-time traffic management and train control for rail networks - part 2: Extensions towards energy-efficient train operations. Transport. Res. Part B: Methodol. 115, 72–94.

NS, 2020. TreinPlein. https://treinplein.net.

ON-TIME, 2014. DAS on-board algorithms. Report D6.3, ON-TIME project.

Peña-Alcaraz, M., Fernandéz, A., Cucala, A., Ramos, A., Pecharromán, R.R., 2012. Optimal underground timetable design based on power flow for maximizing the use of regenerative-braking energy. Proc. Inst. Mech. Eng., Part F: J. Rail Rapid Transit 226 (4), 397–408.

Pengyu, W., Qingnian, W., Wangwei, Naiwei, Z., 2009. The affect of motor efficiency on regenerative braking at low-speed stage. In: 2009 International Conference on Energy and Environment Technology. Vol. 1. pp. 388–391.

Pontryagin, L.S., Boltyanskii, V.G., Gamkrelidze, R.V., Mishchenko, E.F., 1962. The Mathematical Theory of Optimal Processes. Wiley, Hoboken, NY, USA.

Qu, J., Feng, X., Wang, Q., 2014. Real-time trajectory planning for rail transit train considering regenerative energy. In: IEEE 17th International Conference on Intelligent Transportation Systems (ITSC 2014). pp. 2738–2742.

Rao, A.V., Benson, D.A., Darby, C., Patterson, M.A., Francolin, C., Sanders, I., Huntington, G.T., 2010. Algorithm 902: GPOPS, a MATLAB software for solving multiple-phase optimal control problems using the Gauss pseudospectral method. ACM Trans. Math. Software (TOMS) 37 (2), 22:1–22:39.

Ross, I.M., 2015. A Primer on Pontryagin's Principle in Optimal Control. Collegiate Publishers, San Fransisco, CA, USA.

Ross, I.M., Karpenko, M., 2012. A review of pseudospectral optimal control: from theory to flight. Annu. Rev. Control 36 (2), 182–197.

Scheepmaker, G.M., Goverde, R.M.P., 2015. The interplay between energy-efficient train control and scheduled running time supplements. J. Rail Transp. Plan. Manage. 5 (4), 225–239.

Scheepmaker, G.M., Goverde, R.M.P., 2016. Energy-efficient train control including regenerative braking with catenary efficiency. In: IEEE International Conference on Intelligent Rail Transportation, pp. 116–122.

Scheepmaker, G.M., Goverde, R.M.P., Kroon, L.G., 2017. Review of energy-efficient train control and timetabling. Eur. J. Oper. Res. 257 (2), 355–376.

Scheepmaker, G.M., Willeboordse, H.Y., Hoogenraad, J.H., Luijt, R.S., Goverde, R.M.P., 2020. Comparing train driving strategies on multiple key performance indicators. J. Rail Transp. Plann. Manage. 13, 100163.

Steimel, A., 2008. Electric Traction Motive Power and Energy Supply. Oldenbourg Industrieverlag, München, Germany.

Stephan, A., 2008. OpenPowerNet - Simulation of railway power supply systems. WIT Trans. Built Environ. 103, 449–459.

Wang, P., Goverde, R.M.P., 2016. Multiple-phase train trajectory optimization with signalling and operational constraints. Transport. Res. Part C: Emerg. Technol. 69, 255–275.

Yang, S., Wu, J., Yang, X., Sun, H., Gao, Z., 2018. Energy-efficient timetable and speed profile optimization with multi-phase speed limits: Theoretical analysis and application. Appl. Math. Model. 56, 32–50.

Yang, X., Li, X., Gao, Z., Wang, H., Tang, T., 2013. A cooperative scheduling model for timetable optimization in subway systems. IEEE Trans. Intell. Transp. Syst. 14 (1), 438–447.

Yang, X., Li, X., Ning, B., Tang, T., 2016. A survey on energy-efficient train operation for urban rail transit. IEEE Trans. Intell. Transp. Syst. 17 (1), 2–13.

Yang, X., Ning, B., Li, X., Tang, T., 2014. A two-objective timetable optimization model in subway systems. IEEE Trans. Intell. Transp. Syst. 15 (5), 1913–1921.

Yi, S., 2018. Principles of Railway Location and Design. Academic Press, London, UK.

Zhou, Y., Bai, J., Li, J., Mao, B., Li, T., 2018. Integrated optimization on train control and timetable to minimize net energy consumption of metro lines. J. Adv. Transport. 2018, 19.